

Characterization of Endoreplicated Nuclei in *Arabidopsis thaliana*

A Thesis

Submitted to the Graduate Faculty of the
Louisiana State University and
Agricultural and Mechanical College
in partial fulfillment of the
requirements for the degree of
Master of Science

in

The Department of Biological Sciences

by
Rasheed A. Ahmad
B.S., Winona State University, 2003
June 2009

ACKNOWLEDGEMENTS

My thanks and appreciation goes to my advisor and mentor Dr. Naohiro Kato. I am especially grateful for his guidance, patience and understanding throughout my dissertation research. I would have not completed this research without his suggestions, discussions and constant encouragement.

I would like to thank Dr. Anne Grove, Dr. John Larkin, and Dr. Kurt Svoboda for being members of my committee.

I am thankful to Dr. Ingo Schubert and his lab members at the IPK institute, Gatersleben Germany, for their support and collaboration in nuclei sorting.

Above all, I am deeply indebted to my fellow co-workers, Dr. Yukichi Fujikawa, Blake Crochet, Dexter and to my close friends, Mohammad Alshawaf, Mauriciou Marulanda, and Roy Issa for their friendship and support. I also thank Dana Silwadi for peer reviewing my thesis.

TABLE OF CONTENTS

ACKNOWLEDGEMENTS.....	ii
LIST OF TABLES	iv
LIST OF FIGURES	v
ABSTRACT	vi
CHAPTER 1 LITERATURE REVIEW	1
1.1 The Cell-Cycle that Routes to Polyploidization.....	1
1.2 Polyploidization in <i>Homo sapiens</i> , Endomitosis.....	2
1.3 Polyploidization in <i>Drosophila elegans</i> , Polytene Chromosome.....	2
1.4 Polyploidization in <i>Arabidopsis thaliana</i> , Endoreplication.....	3
CHAPTER 2 CHARACTERIZATION OF <i>ARABIDOPSIS</i> ENDOREPLICATED NUCLEI	6
2.1 Introduction	6
2.2 Objectives.....	8
2.3 Materials and Methods.....	9
2.4 Results.....	12
2.5 Discussion	20
CHAPTER 3 LOCALIZATION AND SELF-INTERACTION OF <i>ARABIDOPSIS</i> TOPOISOMERASE VIB	25
3.1 Introduction	25
3.2 Cellular Effects in Mutations of the Topoisomerase VIB Gene in <i>Arabidopsis</i>	27
3.3 Objectives.....	28
3.4 Materials and Methods.....	29
3.5 Results.....	34
3.6 Discussion	43
REFERENCES	45
VITA	50

LIST OF TABLES

Table 1 Sorted Nuclei Collection Methods	16
--	----

LIST OF FIGURES

Figure 1 DAPI Staining Graph of <i>Arabidopsis</i> Nuclei	13
Figure 2 Sorted Nuclei of <i>Arabidopsis</i> Leaves	14
Figure 3 Deconvoluted Images of <i>Arabidopsis thaliana</i> Leaf Tissue 2C, 4C, and 8C Nuclei	17
Figure 4 Comparison of Nuclear Volume between <i>Arabidopsis thaliana</i> 2C, 4C, and 8C Nuclei ...	17
Figure 5 Comparison of Protein Amount between <i>Arabidopsis thaliana</i> 2C, 4C, and 8C Nuclei ...	18
Figure 6 Comparison of RNA Amount between <i>Arabidopsis thaliana</i> 2C, 4C, and 8C Nuclei	19
Figure 7 Type TopIIB Working Scheme	27
Figure 8 Schematic Drawing of AtTopVIB Showing its Domains	35
Figure 9 N-terminal Sequence Alignment of TopVIB	36
Figure 10 C-terminal Sequence Alignment of TopVIB	37
Figure 11 AtTopVIB N-terminal Surface Density Predicted Structure	38
Figure 12 Schematic Drawing of pDuex Vectors Used in the Localization Assay	39
Figure 13 Schematic Drawing of pDuex Vectors Used in the Self-interaction Assay	40
Figure 14 Schematic Drawing of An1RG Showing the YFP Tagged to the N-terminal of Luciferase Clone and Deconvoluted Images of <i>Arabidopsis thaliana</i> Protoplast Transformed with pDuexAn1RG and DAPI Stained	41
Figure 15 Schematic Drawing of An1-AtTopVIB Showing the YFP Tagged to the N-terminal of AtTopVIB Clone and Deconvoluted Images of <i>Arabidopsis thaliana</i> Protoplast Transformed with pDuexAn1-AtTopVIB and DAPI Stained	41
Figure 16 The Average Relative Luminescence Unit in <i>Arabidopsis</i> Protoplast Transformed with pDuexAn6-H2A and pDuexDn6-H2B, or pDuexAn6-AtTopVIB and pDuexDn6-AtTopVIB, or no DNA sample (Mock)	42

ABSTRACT

A model plant, *Arabidopsis thaliana*, duplicates its chromosomes without cell division, in a process known as endoreplication. The primary objective of this study was to identify genes and proteins that specifically accumulate in endoreplicated nuclei in *Arabidopsis thaliana*. Analysis of nuclei sorted by fluorescent activated cell sorter (FACS) revealed that ploidy levels and nuclear volume were positively correlated. However, the protein amounts among 2C, 4C, and 8C nuclei had no significant differences. This indicated a decrease of the protein concentration in endoreplicated nuclei. In contrast, the RNA amount in the 8C nuclei was 1.3- and 1.4-fold higher than that in the 4C and 2C nuclei, respectively. This suggested an increase of RNA after the second round of endoreplication.

The secondary objective was to identify the biological function of unique domains found in *Arabidopsis* topoisomerase VI subunit B (AtTopVIB) that contributes to endoreplication. Using the AtTopVIB amino acid sequence and protein database search engine, I identified two unique domains to which I designated the insertion of the N-terminal domain (IND) and the extension in the C-terminal domain (ECD). These domains are well conserved between *Arabidopsis* and *Oryza sativa* (rice) but very unique in the entire family. Towards understanding the biological function of these domains, I analyzed the localization of AtTopVIB in *Arabidopsis* protoplasts with yellow-fluorescent protein (YFP). The results indicated that AtTopVIB was localized in the nucleus. Also, I analyzed AtTopVIB self interaction in *Arabidopsis* protoplasts using split-luciferase. The results indicated a weak self interaction of AtTopVIB. These results suggested that the IND and ECD may be involved in the localization or self-interaction of AtTopVIB in *Arabidopsis* cells.

CHAPTER 1 LITERATURE REVIEW

1.1 The Cell-Cycle that Routes to Polyploidization

Two of the most fundamental aspects of cells are growth and division. Maintaining an identical copy of genetic material in each cell during cell division is critical in somatic cells. This process is controlled by the cell cycle¹. The plant cell cycle is regulated somewhat differently from other eukaryotes. For instance, plants lack orthologs of the mammalian G₁/S specific cyclin-dependent kinases 4 and 6 (CDK4 and CDK6) but possess a plant specific B-type CDK^{2,3}. Yet they share the main mechanism of regulators controlling the cell cycle transition from one phase to the next⁴. In order for somatic cells to divide, they need to undergo a mitotic cell cycle that results in producing two diploid cells. The mitotic cell cycle encompasses 4 ordered phases, G₁, S, G₂, and M-phase. Although the cell cycle of many eukaryotes requires the successful completion of the M-phase prior to DNA replication in the S-phase, some highly specialized cells skip the M-phase to obtain a polyploid DNA content⁸. For instance, human megakaryocytes skip part of the M-phase (endomitosis), whereas *Arabidopsis* and *Drosophila* specialized cells skip the entire M-phase (endoreplication)^{2,3,6}.

Fausto et al. showed that drugs, such as Chemokine (calcium tetrachloride) that was reported to be toxic to hepatocytes, increased the ploidy level of mammalian hepatocytes which suggests that polyploidization could be a physiological adaptation to cellular stress⁵. Moreover, due to the increase in cell size caused by polyploidization, Otto et al. suggests that polyploidization may be the way to regulate tissue and organ size⁶. In higher plants, polyploidization was shown to be a part of their developmental program and the ploidy level seems to increase with ageing⁷. This case was also observed in diploid hepatocytes in newly born mammals, which increased to tetraploid and octaploid with the ageing process⁸.

1.2 Polyploidization in *Homo sapiens*; Endomitosis

Bone-marrow precursor cells that give rise to blood platelets have a DNA content of up to 128C (C is defined as the DNA content of a haploid nucleus), as opposed to the diploid DNA content of 2C as a result of endomitosis. Endomitosis is a process in which the cell enters mitosis with no nuclear envelope degradation and exiting the M-phase from late anaphase, resulting in an enlarged cell with twice the DNA content per round of cell cycle⁹. The biological function of endomitosis is to produce large megakaryocytes with high ploidy level content which can produce larger number of differentiated platelets compared to diploid megakaryocytes¹⁰. The molecular mechanism of endomitosis owes to the lack of the nuclear envelope degradation in prophase and is due to the lack of proteins, such as the Aurora B Kinase, involved in the formation of a network of anti-parallel microtubules between the separating chromosomes during the metaphase/anaphase transition¹¹.

1.3 Polyploidization in *Drosophila elegans*; Polytene Chromosome

In the salivary gland of the fruit fly *Drosophila* this endoreplicated nuclei have puffed polytene chromosomes following S-phase with visible light and dark bands under the microscope¹². The dark bands represent areas of the genome that are densely packed, whereas the light bands represent areas of the genome that are lightly packed. The puffs represent transcriptionally active genes in the genome¹². The sister chromatids stay aligned throughout the cell cycle until the proceeding S-phase¹³. Although the precise function of forming polytene chromosome is still unknown, it has been proposed that it occurs in highly specialized cells that demand higher protein content to carry on their required function¹⁴.

It has been reported that there is a significant under-presentation of the heterochromatin DNA in duplicated genomes in salivary gland cells of *Drosophila*^{15,16}. This is at least partially

due to the oscillation of cyclin E (CycE) levels during the G₁-S phase transition¹⁶. CycE is a regulator of G₁ to S-phase transition in mammalian cells¹⁷. The control of CycE levels during the endocycles is regulated by an E3 ubiquitin ligase that transfers a ubiquitin molecule from the cysteine of E2 ubiquitin-conjugated enzyme, to the lysine of the target protein for proteolysis by the proteasome^{18,19}. Hence, the hypomorphic P-element mutation of CycE (*CycE¹⁶⁷²*) allows the completion of the genomic duplication including the replication of the late heterochromatin in *Drosophila* ovarian cells¹⁵.

1.4 Polyploidization in *Arabidopsis thaliana*, Endoreplication

Zuzana et al. suggested that endoreplication occurs in organisms with a small genome size to increase their gene expression activity yielding higher protein content needed to carry on their specialized function²⁰. Melaragno et al. also suggested that endoreplication is part of a developmental program in *Arabidopsis*²¹.

Unlike *Drosophila* salivary gland cells, *Arabidopsis* specialized cells, such as pavement leaf cells and trichomes, undergo endoreplication producing uncondensed chromatin with no visible puffs or bands. Morphological difference in the DNA between *Drosophila* polytene chromosomes and *Arabidopsis* endoreplicated chromosomes suggests a difference in the mechanism of chromosome sorting, decatenation, and chromosome condensation post replication.

Cyclin dependent kinase B1;1 (CDKB1;1) is a key regulator of the transition from G₂ to the M-phase by interacting with cyclin A3;2 (CYCA3;2), cyclin A2;3 (CYCA2;3), and cyclin D3;1 (CYCD3;1) in *Arabidopsis*. It is known that CDKB1;1 is highly expressed in dividing cells and is down regulated at the onset of endoreplication²². Also, transgenic *Arabidopsis* overproducing a dominant negative CDKB1;1 undergo increased endoreplication²². Hence,

CDKB1;1 is considered the key molecule that control endoreplication in *Arabidopsis*. Another CDKB found to control endoreplication is the CDKB1;2. Ectopic expression of CDKB1;2 switches the developmental fate of *Arabidopsis* trichomes from endoreplicating into mitotically dividing cells²³. A different molecule that is also known to control the switch from the mitotic cycle to endoreplication is CCS52A, an ortholog of the yeast and animal *cdh1/srw1/fzr* genes acting as a substrate-specific activator of the anaphase-promoting complex (APC) ubiquitin ligase. The CCS52A controls the degradation of mitotic cyclins²⁴. It has been reported that the down regulation of CCS52A significantly reduces the ploidy level in *M.truncatula* nodules²⁵. Also, it has been reported that mis-expression of one of the three identified CCS52A genes (*fzr-1*, *fzr-2*, *fzr-3*), *fzr-2*, is sufficient to drive endoreplication in *Arabidopsis* petals²⁶. Also, a T-DNA insertion in the *fzr-2* gene (*fzr2-1*) in *Arabidopsis* resulted in smaller leaf cells that undergo fewer endoreplication cycles²⁶. This suggests that CCS52A plays a role in regulating the developmental control between mitotic cycles and endoreplication.

Another gene that controls endoreplication and is involved in cell cycle regulation is the SIAMESE (SIM). SIM function was reported to repress the mitotic division by interacting with the regulators of G₁ to S phase transition, D-type cyclins (CycD) and cyclin-dependent kinase A;1 (CDKA;1), in *Arabidopsis*²⁷. Mutations in SIM of *Arabidopsis thaliana* resulted in multicellular trichomes that encompass single nuclei with a low ploidy level, a phenotype strikingly different from that of wild-type trichomes²⁷. Moreover, over-expression of SIM causes enlarged epidermal cells with higher DNA content due to increase in the number of endocycles in *Arabidopsis thaliana*²⁷.

Other genes that are not involved in cell cycle regulation but control endoreplication in *Arabidopsis* have been identified. These genes include *rh11*, *rh12*, *hyp6*, *bin4*, and *midget* all of

which constitutes the topoisomerase VI complex in *Arabidopsis*. Mutations in those genes resulted in a similar phenotype of dwarf plants with reduced ploidy levels and smaller cell size^{33,28,32,34}. However, the mechanism by which the topoisomerase causes endoreplication is not clear.

CHAPTER 2 CHARACTERIZATION OF *ARABIDOPSIS* ENDOREPLICATED NUCLEI

2.1 Introduction

Kato et al. established an *Arabidopsis thaliana* transgenic plant *EL702C* that has GFP/lacI cassette integrated in two loci 4.2 Mbp apart on chromosome 3. The *EL702C* transgenic plant was used to compare the chromosome movement in diploid and endoreplicated nuclei by measuring the overall mean squared change in distance over the change in time between the 2 inserted loci. The results showed that the change in distance squared over the elapsed time in endoreplicated nuclei was significantly higher compared to diploid nuclei²⁹. These results suggest a loss or modification in the protein content of *Arabidopsis* endoreplicated nucleus. Attachment of the chromatin to the nuclear envelope is controlled by scaffold proteins, known as lamin proteins, in animals³⁰. In higher plants a nuclear matrix-localized protein (MFP1) carrying a coiled-coil motif that binds to the nuclear matrix attachment regions of the chromatin (MAR) has been identified³¹. Kato et al. raised the question of what could cause such behavior inside the endoreplicated nucleus.

Mutational studies of genes such as *rh11*, *mid*, and *bin4*, all of which are members of the topoisomerase VI complex in *Arabidopsis thaliana*, identified a clear phenotype with reduced endoreplication levels. Interestingly, none of these mutants eliminated the endoreplication process completely and the plant still carried nuclei with ploidy level up to 8C in their leaf tissues^{32,33,34}. This suggests that the first two cycles of endoreplication may be essential for embryo development.

A microarray analysis comparing the gene expression patterns between *Arabidopsis thaliana* diploid and synthetic allopolyploid (formed by pollinating an autotetraploid species

with another autotetraploid species) established by interspecific hybridization between autotetraploid *Arabidopsis thaliana* and *Arabidopsis arenosa* was reported. Among approximately 2430 cDNA studied, 11% displayed a change in expression in the S2-S4 (allotetraploid line self crossed for 3 generations) progenitors, compared to both parents. Approximately 40 genes that are highly expressed in the parent *Arabidopsis thaliana* were further analyzed to their expression rate in the progenitor. These genes encode proteins involved in cell metabolism, cell division, protein transport, signal transduction, and transposons. Among these genes 26 (60%) are down-regulated³⁵. They also reported that this down-regulation is caused by methylation on the chromosomes³⁵. These silenced genes are thought to be unnecessary in allopolyploid cells. Overall, this study showed a unique expression pattern in a synthetic allotetraploid compared to *Arabidopsis thaliana* diploid seedlings suggesting a difference in expression pattern between diploid and allopolyploid cells.

The studies mentioned above indicated that endoreplicated cells/nuclei may contain their specific proteins and RNAs so that their biological function is specialized. Our goal was to identify these proteins and RNAs that may be specifically accumulated in endoreplicated nuclei to understand the biological function of endoreplication. A challenge to identify endoreplicated-nuclei-specific proteins and RNAs is that a high number of nuclei are required to obtain enough amounts of nuclear protein and RNA for downstream analysis. Galbraith et al. established a nuclei sorting technique that yields a significantly high number of sorted nuclei compared to other techniques such as the quantitative microphotometry that uses DNA specific dyes without sorting³⁶. Their method allows for the sorting of nuclei according to their DNA content using a Fluorescence Activated Cell Sorter (FACS)³⁶.

2.2 Objectives

Objective I: Optimizing the Condition to Collect the Sorted Nuclei

The method developed by Galbraith et al sorts 10^6 *Arabidopsis thaliana* nuclei in 10 mL of Nuclei Sorting Buffer (NSB). I needed to concentrate the sorted nuclei from a volume of 10mL into smaller volumes of 100-200 μ L to obtain enough amounts of protein and RNA to identify the nuclear proteins and genes in endoreplicated nuclei. I used several approaches to concentrate the sorted nuclei while preserving the integrity of its content.

Objective II: Measuring *Arabidopsis thaliana* Nuclear Volume, Protein, and RNA amounts of Endoreplicated Nuclei

I wanted to determine the actual nuclear volumes, and the actual amount of proteins and RNAs in endoreplicated nuclei. Therefore, I compared the nuclear volume and the amounts of proteins and RNAs between diploid and endoreplicated nuclei. I hypothesized that *Arabidopsis thaliana* endoreplicated nuclei have higher protein and RNA levels than diploid nuclei.

Objective III. Comparing the Protein and mRNA Content between Diploid and Endoreplicated Nuclei by iTRAQ and Microarray Analysis

I hypothesized that there is a difference in the nuclear protein content between diploid and polyploidy nuclei in *Arabidopsis thaliana*. I predicted that some proteins are biochemically modified in endoreplicated nuclei causing the less restricted movement of the chromosomes. To compare the protein content between diploid and endoreplicated nuclei I decided to use the isobaric tag for relative and absolute quantification (iTRAQ) due to its comparative and rapid results. The iTRAQ can compare up to 4 distinct samples simultaneously. After labeling the different protein samples with the isobaric tags, dual mass spectrometry (MS/MS) fragmentation gives the distinct reporter ions that are used to quantify their respective samples. The iTRAQ test

requires 50-100 µg of protein per studied sample (diploid vs. endoreplicated) at a concentration of 2.5 µg/µL.

It is also possible that some mRNAs are specifically accumulated in endoreplicated nuclei in *Arabidopsis*. To compare the RNA content between diploid and endoreplicated nuclei I decided to use the oligonucleotide microarray services offered by the David Galbraith lab at Arizona State University. The microarray analysis requires 200 ng per ploidy level as a minimum amount of total RNA per studied sample at a concentration of 20 ng/µL.

2.3 Materials and Methods

- **Nuclei Sorting**

Arabidopsis thaliana Columbia ecotype was grown in long-day growth chamber (16 hrs of light/8hr of dark). Leaves of 3 weeks old plants were chopped in a cold room with a single edged razor blade in a glass petri-dish (diameter, 5 cm) containing a Nuclei Sorting Buffer (NSB). The NSB contents: 45 mM magnesium chloride, 30 mM sodium citrate, 20 mM 3-morpholinopropanesulfonic acid (MOPS), and Triton X- 100(1 mg/ml) at pH 7.0. The chopped leaf suspension was then passed through a 50 µm nylon mesh and centrifuged at 500 x g for 3 minutes. The pellet was re-suspended in 5 mL of NSB containing 2 µl of 4',6-diamidino-2-phenylindole (DAPI) (100 µg/mL). For sorting, a fluorescence activated cell sorter (FACStar^{Plus}, Beckton Dickinson, Germany) with a 70 µm size nozzle equipped with an Argon-ion laser (INNOVA 90C-5) emitting UV-light was used. 10⁵ DAPI stained nuclei was sorted to collect 2C, 4C, and 8C nuclei in 10mL NSB. Light microscopy equipped with DAPI filter was used to confirm the presence of sorted nuclei.

- **Collecting the Sorted Nuclei**

For collecting the sorted nuclei, 10⁵ nuclei of 2C, 4C, and 8C ploidy in 10 mL NSB was centrifuged at different speeds and times. Initially, 10 mL of 2C sorted nuclei were centrifuged at

850 x g for 10 min at 4°C as suggested by Meier et al.³⁷. Twenty microliters of the centrifuged nuclei solution was stained with DAPI (100 µg/mL) and used to quantify the nuclei number using fluorescent microscope equipped with DAPI filter and a hemocytometer. In addition to this conventional method, the following methods were employed to collect the sorted nuclei.

1. Ten milli-liters of 2C sorted nuclei was passed once through a 40 µm and another through 100 µm nylon mesh (Amicon-ultra Inc., USA). Twenty microliters of the filtrate and the flow-through were stained with DAPI and used to quantify the nuclei number.
2. Ten milli-liters of 2C sorted nuclei was added to a10 kDa Millipore tubes (Millipore Inc., USA), which recover proteins with molecular weight higher than 10 kDa, and spun at 3,800 x g for 40 minutes at 4°C.
3. Ten milli-liters of 2C sorted nuclei was added in a 1:1 molar ratio to Gold nanoparticles colloid that has been reported to bind nuclear membrane proteins of low abundance (Sigmaaldrich Inc., USA) and incubated over night at 4°C³⁸. This was followed by two steps of centrifugation at 3,800 x g for 40 min at 4 °C and washing with a 4-(2-hydroxyethyl)-1-piperazineethanesulfonic acid (HEPES) buffer. Twenty microliters of the resulting pellet was stained with DAPI and used to quantify the nuclei number.
4. Eventually, 2C sorted nuclei were collected using an ultra-centrifuge by spinning the 10mL NSB containing the sorted nuclei at 22,000 x g for 2 hours at 4°C. This was followed by re-suspending the nuclei pellet in 100 µL of nuclei lysing buffer (NLB 20 mM KCl, 20 mM HEPES, pH 7.4, 0.6%(v/v) Triton X-100, 13.8% (v/v) hexylene glycol, 1% (v/v) thioglycol, 50 µM spermine, 125 µM spermidine, 1 mM

Phenylmethylsulfonyl fluoride (PMSF), 2 $\mu\text{g}/\mu\text{L}$ aprotinin) for protein and RNA quantification.

- **Measuring Nuclei Volume**

Sorted nuclei were stained with DAPI (10 $\mu\text{g}/\mu\text{L}$) and viewed under a 100X oil-immersion objective of a de-convolution microscope (Leica DM RXA2, Leica Microsystems, USA). Sorted nuclei volume was calculated by analyzing an acquired image stack using deconvolution microscopy. Stacking on images were taken and the image was subjected to convolution to remove any optical distortion. Image analysis and constrained iterative deconvolution were performed with the software Slidebook version (Intelligent Imaging Innovation, USA).

- **Protein Quantification**

For nuclear protein quantification, 4 bovine serum albumin (BSA) (SigmaAldrich Inc., USA) aliquots with concentrations ranging from 0-50 $\text{ng}/\mu\text{L}$ made with dH_2O were prepared. One microliter of each BSA aliquot was suspended in 1 mL of the dye solution provided by the Bradford kit (Bio-rad Inc., USA) that binds non-covalently to hydrophobic regions of proteins. One milliliter of dye solution with no protein sample was used to blank the light spectrophotometer (Thermo-Scientific, USA). Absorbance of BSA aliquots was measured at 595 nm. A BSA standard curve for protein quantification was established. This was followed by suspending 1 μL of the lysed nuclei solution in 1 mL of the dye solution and measuring the absorbance.

- **RNA Quantification**

For nuclear RNA quantification, 10 μL of RNase A inhibitor (10 $\mu\text{g}/\text{mL}$) was added to 100 μL solution containing the lysed nuclei, releasing the nuclear RNA content in to the solution. Twenty micro liters of two RNA quantification standards (0 $\text{ng}/\mu\text{L}$ and 100 $\text{ng}/\mu\text{l}$) were

suspended in 180 μL reaction mix provided by the Qubit kit (Invitrogen Inc., USA), and used to blank the spectrophotometer. Nuclear RNA content was quantified by suspending 1 μl of the lysed nuclei solution in 199 μL of the reaction mix and measuring the fluorescence, that bind specifically to RNA, using a spectrophotometer provided by the same kit.

2.4 Results

Nuclei Sorting

In an attempt to obtain enough amounts of proteins and RNA for the downstream analysis, approximately 5×10^6 nuclei were collected from approximately 6000 leaves of 3 week old *Arabidopsis* at the Genomic Institute (IPK) in Gatersleben, Germany. The leaves were directly chopped by a razor blade in the nuclei sorting buffer (NSB). In my conditions, 5×10^5 nuclei of different ploidy levels were released from 600 leaves in about 50 mL NSB. The nuclei were then stained with 4',6-diamidino-2-phenylindole (DAPI) and placed in a fluorescence activated cell sorter (FACS). DAPI stained nuclei generate forward light scatter (FSC) during sorting (Fig. 1). This data helps in defining the timing of gate opening to sort the nuclei into different ploidy levels (2C, 4C, 8C, 16C, and 32C). About 10 hours were taken to sort 5×10^5 nuclei. Sorted nuclei were then collected in 10 mL NSB depending on their ploidy levels (2C, 4C, and 8C). The histogram in Figure 2 shows the ploidy level of sorted nuclei, the number of sorted nuclei (labeled as events), and their corresponding DAPI intensities (labeled as Violet-1A) (Fig. 2). In summary, 10 tubes for each ploidy level (each tube containing 10^5 nuclei), total of 100 mL, were collected over a period of 10 days (100 h). The tubes were immediately frozen in liquid nitrogen, stored at -80°C and shipped to Louisiana State University.

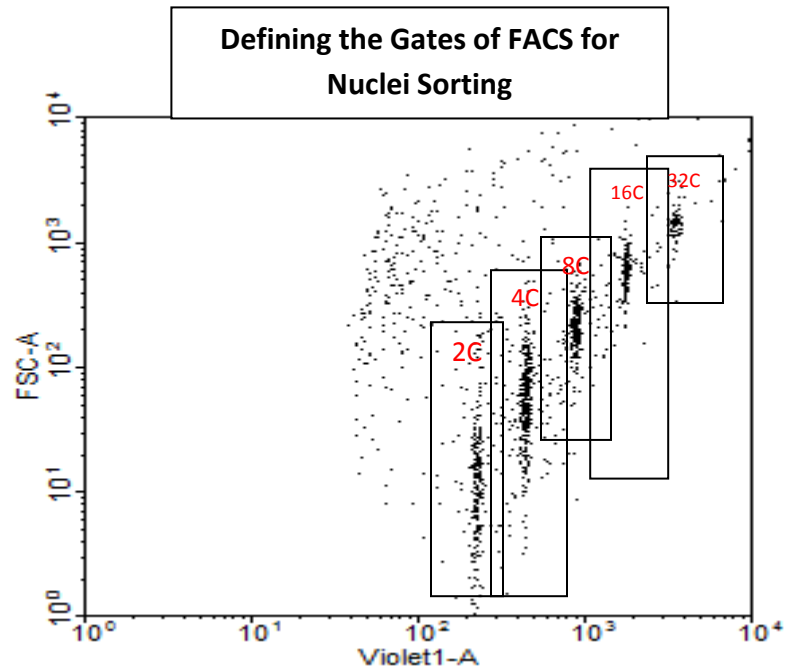


Figure 1. DAPI staining graph of *Arabidopsis* nuclei. This information was used to determine the timing of gate opening for nuclei with different ploidy levels (each rectangle represents a different gate). Y-axis shows the forward light scatter (FSC) and the x-axis shows the intensity of DAPI fluorescence (labeled as Violet1-A).

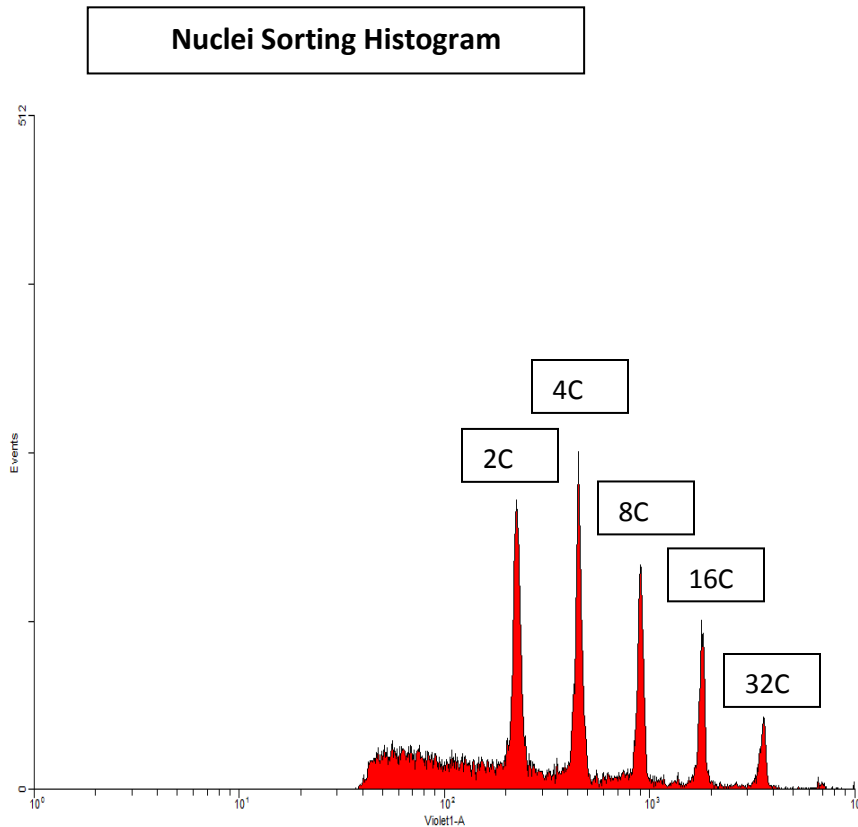


Figure 2. The sorted nuclei of *Arabidopsis* leaves. The flow cytometric histogram shows the nuclei ploidy level, number of nuclei sorted (labeled as events on the y-axis), and its corresponding DAPI intensity is detected from a total of 5×10^5 nuclei (labeled as Violet-1A on the x-axis).

Concentration of Sorted Nuclei

To conduct the iTRAQ assay, 50-100 μg of protein at a concentration of 2.5 $\mu\text{g}/\mu\text{L}$ is required³⁹ (personnel communication, W.M. Keck Foundation, Biotech Resource Laboratory Yale University, USA). To conduct the microarray assay, 200 ng of total RNA at a concentration of 20 $\text{ng}/\mu\text{L}$ of total RNA is required⁴⁰ (personnel communication, Dr. Galbraith Arizona State University, USA). Hence, I concentrated the sorted nuclei into smaller volume of (100-200 μl) NSB so that I could extract those molecules at the most efficient manner. Five different methods were used to concentrate the sorted nuclei because a conventional nuclei concentration technique using a centrifuge at 850 x g for 10 min at 4 °C did not precipitate enough nuclei under my conditions (Table 1). The number of precipitated nuclei was calculated by staining the precipitate with DAPI and then counting the nuclei number using a microscope equipped with a DAPI filter

and a hemocytometer. Using 10^5 sorted nuclei in 10 mL of NSB as a starting material, centrifugation at $850 \times g$ precipitated only 10^2 nuclei, or 0.1% of the starting material. This number was not enough to obtain enough protein and RNA for the downstream analysis [This is most likely due to electrostatic charges of sorted nuclei (Dr. D. W. Galbraith, personal communication)]. Hence, I used four other methods to collect the sorted nuclei. Knowing that *Arabidopsis* nucleus size is about $10\text{-}200 \mu\text{m}^2$ ²¹, I passed the sorted nuclei solution through a $40 \mu\text{m}$ filter membrane. However, the solution did not pass through the filter membrane; perhaps the nuclei clogged the pores of the filter membrane. Alternatively, I used a larger pore size of $100 \mu\text{m}$ filter membrane. Though the solution went through the filter membrane, the number of nuclei that remained on the membrane filter was only 10^3 , or 1% of the starting material. Hence, the membrane filter method did not concentrate the nuclei enough to extract the protein and RNA efficiently. The Millipore centrifugal filter with a molecular weight cut-off of 10 kDa (Amicon Ultra-15, Millipore, USA), known to concentrate proteins was also used to concentrate the nuclei. When adding the solution containing the sorted nuclei to the Millipore filter the solution turned blue. Although I did not know the actual reason, it might be a chemical reaction between the NSB ingredients and the Millipore filter. Therefore, I was not able to use this method to collect my sorted nuclei. Gold nano-particles (AuNP) method has been reported to bind to and concentrate low abundance proteins needed for proteomic analysis³⁸. Hence, I tried to concentrate the sorted nuclei by binding to the AuNP and then precipitating the nuclei bound to AuNP. The AuNP (Sigma Aldrich, USA) precipitation protocol was adopted from Wang et al.³⁸ and was used to precipitate the 10^5 sorted nuclei. However the recovered nuclei using the AuNP's method was only 10^3 , or 1% of the starting material.

Since none of the methods mentioned above recovered the amounts of nuclei needed to

extract protein and RNA for my downstream analysis, as the last method, I spun the sorted nuclei at a maximum speed of 22,000 x g for 2 hrs at 4°C using an ultra-centrifuge. One drawback of this method was that the membrane of precipitated nuclei was ruptured. This may cause the loss of nuclear protein and RNA. Although I could not count the number of nuclei, due to disturbed structures of the precipitated nuclei, I was able to collect enough RNA (200 ng) to carry on the microarray assay. However, the recovered amount of protein (3.6 µg) was not enough to carry on the iTRAQ analysis.

Table 1. Sorted nuclei collection methods along with the starting nuclei number and the recovered nuclei number of each collection method (N/M not measured).

Collection Method	Centrifugation at 850 x g for 10 min.	Filtration using 40 µm filter membrane	Filtration using 100 µm filter membrane	Millipore tube centrifugation 4,852 x g for 30 min.	Gold nano-particles centrifugation 4,852 x g for 40 min.	Ultra-centrifugation at 22,000 x g for 2 hrs.
Starting Nuclei Number	10 ⁵ /10 mL	10 ⁵ /10 mL	10 ⁵ /10 mL	10 ⁵ /10 mL	10 ⁵ /10 mL	10 ⁵ /10 mL
Ploidy level Used	2C	2C	2C	2C	2C	2C
Recovered Nuclei Number	10 ² /100 µL	N/M	10 ³ /10 mL	N/M	10 ³ /100 µL	N/M
Recovered RNA	N/M	N/M	N/M	N/M	N/M	20 ng/µL

Evaluation of Sorted Nuclei

Nuclei Volume

To compare the nuclear volumes of endoreplicated nuclei, the sorted nuclei were stained with DAPI before the centrifugation and viewed under a deconvolution fluorescent microscope equipped with DAPI filter (Fig. 3). The nuclei were counted using a hemocytometer. Images of ten DAPI stained nuclei from 2C, 4C, and 8C sorted pools were captured with the deconvolution fluorescent microscope showing the positive correlation between ploidy level and nuclei size.

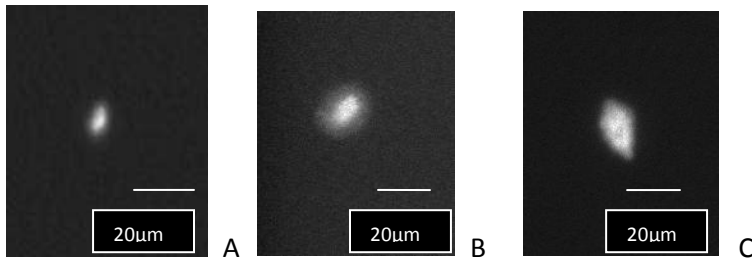


Figure 3. Deconvoluted images of *Arabidopsis thaliana* leaf tissue A) 2C nucleus, B) 4C nucleus, and C) 8C nucleus stained with DAPI.

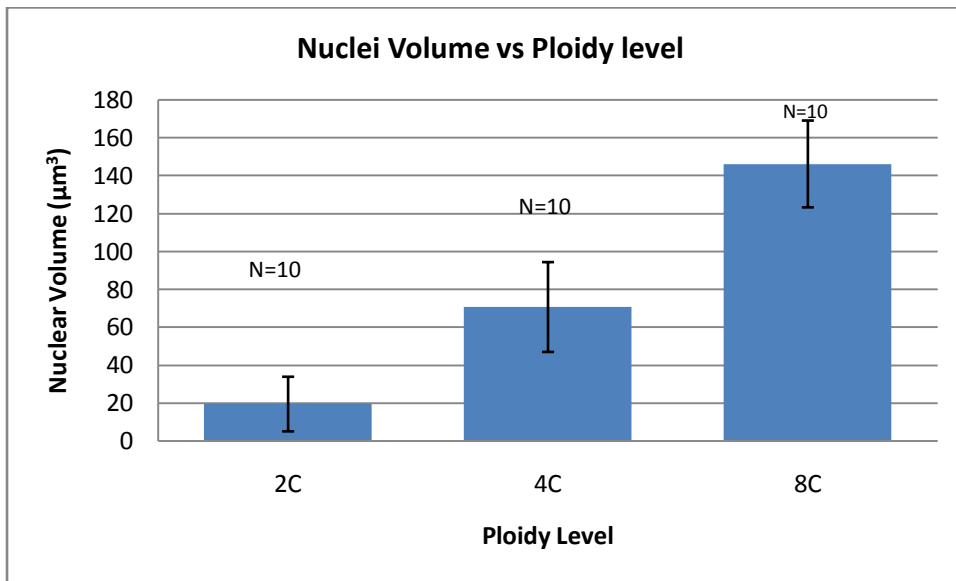


Figure 4. Nuclear volume comparison of 2C, 4C, and 8C sorted nuclei of *Arabidopsis thaliana* leaf tissue (N is the number of nuclei used to calculate the nuclear volume for each ploidy level). Error bars represents standard deviation.

The average nuclear volume from 10 nuclei of 2C, 4C, and 8C sorted nuclei was calculated using the deconvolution microscopy. The analysis revealed an average volume of 19.47 ± 14.42 , 70.70 ± 23.71 , and $146.26 \pm 20.92 \mu\text{m}^3$ in 2C, 4C, and 8C nuclei, respectively (Fig. 4). This suggested the positive correlation between the ploidy level and the nuclear volume of the sorted nuclei.

Nuclear Protein Quantification

In order to quantify the amount of protein in the sorted nuclei, I lysed the nuclei collected

by the ultra-centrifuge method in 100 μL of nuclei lysing buffer (NLB). This lysing step allowed for the release of the nuclear protein content for quantification. One microliter of the re-suspended pellet was used to quantify the nuclear protein amount using the Bradford assay kit (Biorad, USA). Bovine serum albumin (BSA) was used as a standard protein to derive a standard curve for each protein quantification test (data not shown). Nuclear protein quantification of three separate tests of 2C, 4C, and 8C sorted nuclei resulted in 35.13 ± 2.1 , 37.03 ± 2.3 , and 36.07 ± 2.16 $\text{ng}/\mu\text{L}$, respectively. Because 10^5 nuclei were precipitated and re-suspended in 100 μL of NLB, I concluded that each nucleus of 2C, 4C, and 8C had 35, 37, and 36 pg of protein respectively (Fig. 5). This result indicated that there is no significant difference in the protein amount of 2C, 4C, and 8C nuclei (Fig. 5).

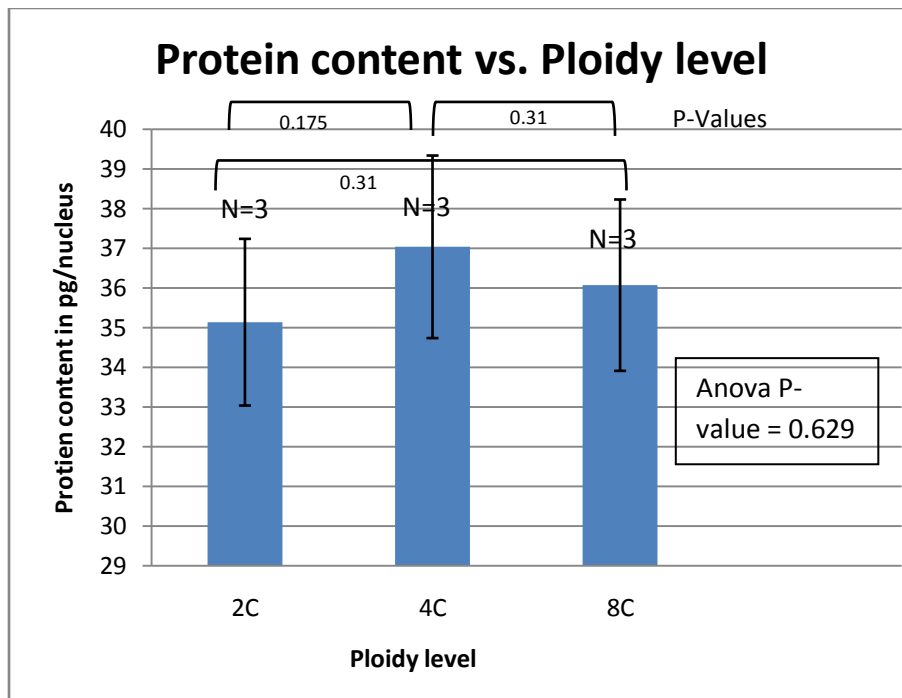


Figure 5. Comparison of the average protein amounts between 2C, 4C, and 8C sorted nuclei of *Arabidopsis thaliana* leaf tissue and their corresponding t-test and Anova (analysis of variance) p-values (N is the number of times the experiment was repeated).

Nuclear RNA Quantification

In order to quantify the amount of total nuclear RNA, I lysed the nuclei collected by the ultra-centrifuge method in 100 μL of nuclei lysing buffer (NLB). To prevent the degradation of the RNA, I also added RNase A inhibitor (10 $\mu\text{g}/\mu\text{L}$) to the NLB. This lysing step allowed for the release of the total nuclear RNA content for quantification. One micro liter of the re-suspended pellet was used to quantify the total nuclear RNA using the Qubit kit (Invitrogen Inc., USA). Two standards (0 $\text{ng}/\mu\text{L}$ and 10 $\text{ng}/\mu\text{L}$) were used as a standard RNA to derive the standard curve for each RNA quantification test. Nuclear RNA quantification of three separate tests of sorted nuclei resulted in 18.1 ± 2.1 , 20.3 ± 2.2 , and 26.1 ± 1.28 $\text{ng}/\mu\text{L}$ in 2C, 4C, and 8C, respectively. Because 10^5 nuclei were re-suspended in 100 μL of NLB, I concluded that each nucleus of 2C, 4C, and 8C had 18, 20, and 26 pg of total RNA respectively. This result suggests that the RNA content of 8C nuclei showed a 1.3- and a 1.4-fold increase in comparison to 2C and 4C nuclear RNA content respectively (Fig. 6). No significant difference between 2C and 4C nuclear RNA was detected (p-value > 0.089).

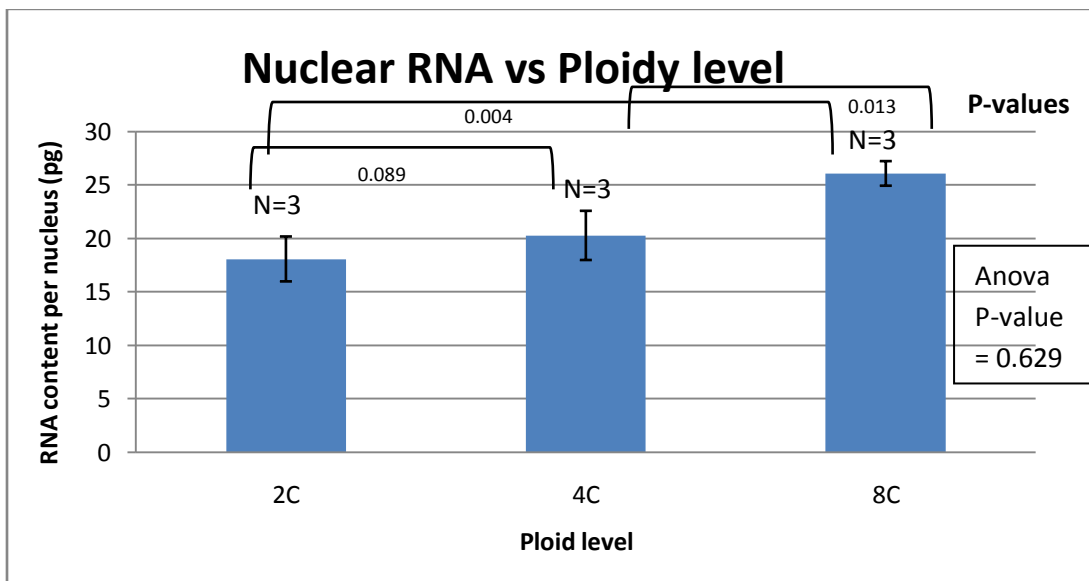


Figure 6. Comparison of average nuclear RNA amounts between 2C, 4C, and 8C sorted nuclei of *Arabidopsis thaliana* leaf tissue and their corresponding t-test and Anova (analysis of variance) p-values (N is the number of times the experiment was repeated). Error bars represents standard deviation.

iTRAQ and Microarray Analysis

In order to conduct the iTRAQ analysis I needed 50-100 μg of nuclear protein per ploidy level at a concentration of 2.5 $\mu\text{g}/\mu\text{L}$. Based on the analysis of nuclear protein quantification, I could only collect about 3.5 μg of nuclear protein per ploidy level. This meant that I would need about 100 tubes of sorted nuclei per ploidy level (each tube having 10^5 of sorted nuclei) to collect enough nuclear protein to conduct the iTRAQ analysis. Hence, I was not able to conduct the iTRAQ analysis.

In order to conduct the microarray analysis I needed 200 ng of total RNA at a concentration of 20 $\text{ng}/\mu\text{L}$. Based on the analysis of nuclear RNA quantification, I collected about 200 ng of total nuclear RNA per ploidy level of sorted nuclei. The total RNA extracted from 2C nuclei and 8C nuclei was then sent to Arizona State University (ASU) for microarray analysis. At ASU, the mRNA was tagged with a fluorescence probe from the RNA provided to check the quality of the mRNA. No fluorescence labeled mRNA was detected which suggests the poor quality of the extracted RNA (Dr. J. Janda, personal communication). Hence, I was not able to conduct the microarray assay.

2.5 Discussion

I have extracted and sorted nuclei from *Arabidopsis thaliana* leaf tissues into 2C, 4C, and 8C ploidy pools. The analysis of nuclei volume by the deconvolution microscopy revealed the positive correlation between ploidy level and nuclei volume. These results agree with a report by Jovtchev et al⁴¹ that shows the positive correlation among ploidy level, cell volume, and nuclear volume in *Arabidopsis thaliana*⁴¹. Moreover, these results support the hypothesis that endoreplication is related to an evolutionary adaptation resulting in an increase in cellular growth in organisms that carry a small genome in order to carry on the required cellular metabolic

functions. Another explanation for such a correlation is that the genome duplication in endoreplicated nuclei needs double the nuclear volume of diploid nuclei to preserve the corresponding space for chromatin thus triggering the expansion of the nuclear volume. Interestingly for me, the volume of 4C nuclei was 3 fold higher than 2C nuclei different than the 2 fold increase reported. However, Schubert et al. showed that endoreplicated chromosomes of *Arabidopsis thaliana* cohere together at random positions and hence, do not need the extra space created by the increased nuclear volume⁴². This finding raised the question as to why do endoreplicated cells increase their nuclear volume if the endoreplicated chromosomes cohere so often.

The protein amounts of 2C, 4C, and 8C nuclei showed no significant difference among them. Together with the results of the nuclei volume analysis, suggests a decrease in protein concentration in these endoreplicated nuclei. These decreases in protein concentration were surprising, since the hypothesis for the cause of endoreplication in *Arabidopsis* is to increase the protein content of the cell and nucleus to carry out its required function. One explanation for this decrease of protein concentration in endoreplicated nuclei is the specific over-replication of the heterochromatin region, a chromatin region with highly repetitive sequence. Because this region rarely expresses genes encoding proteins, endoreplicated nuclei may have similar protein amounts to diploid nuclei. Because polytene chromosomes of follicle cells in *Drosophila melanogaster* have lower copies of heterochromatin compared to euchromatin regions⁴³, I speculate that *Arabidopsis* may undergo re-replication in heterochromatin regions as opposed to *Drosophila melanogaster*.

Another explanation for the decrease in the protein concentration of endoreplicated nuclei may be due to the gene silencing of the endoreplicated copy by epigenetic means that leads to the

inhibition of protein expression. Some genes in *Arabidopsis* synthetic allotetraploids are down-regulated due to hypermethylation of those genes³⁵. This may suggest that an epigenetic mechanism is involved in controlling the expression of specific genes in the endoreplicated nuclei.

I do not deny the possibility that the similar protein amounts in 2C, 4C, and 8C nuclei may owe to the collecting method I used. Spinning the sorted nuclei at such high speeds (22,000 x g) could cause the rupture of the nuclear membrane, and release the soluble nuclear proteins into the NSB. This may result in the loss of nuclear proteins. If this is the case, then it explains the insignificant difference between the protein amounts among 2C, 4C, and 8C nuclei. If this is the case, it is possible that the concentration of nuclear membrane proteins may be reduced in the endoreplicated nuclei.

In 2C and 4C nuclei there was no difference in the amount of nuclear RNAs. This suggests a decrease in the RNA concentration since the nuclear volume tripled. One explanation for this may be due to transcription inhibition of the re-replicated genome. It may be suggested that the transcription is regulated either by epigenetic mechanism such as DNA methylation, or by regulation of the transcription factors involved in transcription initiation. However, I can not rule out the possibility that RNAs are lost during the nuclei collection method.

DNA methylation in *Arabidopsis thaliana* is mainly achieved by DNA methyltransferase (MET1)⁴⁴. Met1 was also found to be responsible in gene down-regulation in synthetic allotetraploids³⁵. Therefore, met1 expression may be up-regulated and that up-regulation of met1 is responsible, at least partially, for transcription silencing of the 4C nuclei genome in the first round of the endocycle.

Arabidopsis thaliana encompasses approximately 1,572 genes that encode for

transcription factors, 6% of the total number of genes⁴⁵. One common transcription factor family in *Arabidopsis* is E2F. E2F regulates the G₁ to S-phase transition during the cell cycle by either binding to its dimerization partner (DP) that allows the transcription of genes required for the S phase or by binding to the Retinoblastoma (Rb) preventing it from interacting with the transcription machinery and thus preventing G₁ to S-phase transition⁴⁶. Therefore, it is possible that the similarity of the nuclear RNA content between 2C and 4C nuclei may be due to the regulatory mechanism of transcription factor that inhibits transcription in 4C nuclei although they encompass double the DNA amount found in 2C nuclei.

Similar RNA amounts in 2C and 4C nuclei may be due to the up-regulation of gene expression that is initiated in nuclei with ploidy levels of 8C and higher. In support of this hypothesis, most genes identified by mutational studies to play a role in endoreplication have affected the second and third rounds endocycles but not the first^{32,33,34}.

In 8C nuclei a 1.4- and 1.3-fold increase in the total nuclear RNA amount was seen compared to 2C and 4C, respectively. This increase in the total nuclear RNA may be due to an increase in either the heterochromatic region of the chromatin that encodes for ribosomal RNA (rRNA), since it constitutes the majority of the total cellular RNA, or due to an increase in the mRNA encoding proteins.

rRNA is clustered in heterochromatic nucleolus-organizing regions known as NOR2 and NOR4 on chromosomes 2 and 4 respectively. Therefore, an increase in the rRNA transcription may increase the total RNA amount. However, the transcription of rRNA has been reported to be massive-energy consuming compared to the transcription of other parts of the genome⁴⁷. This contradicts the hypothesis that cells exit the cell cycle and undergo endoreplication to conserve

energy²⁰. Hence, it is possible that *Arabidopsis* may have adapted strategies, cell proliferation and cell expansion in its developmental program, which in any case requires energy.

Alternatively, the increase in total nuclear RNA content may owe to an increase in mRNA. Based on my protein quantification analysis, I suggest that if mRNA increases in 8C nuclei it would most likely encode for non-nuclear proteins. This would make endoreplicating cells have higher gene expression encoding cytoplasmic proteins that may be involved in the cell expansion.

The similar nuclear RNA amount seen between 2C and 4C nuclei and then the increase in nuclear RNA content in 8C nuclei adds to the ambiguity of the endoreplication function. Whereas I expected to see a positive correlation between nuclear RNA and nuclear volume, for the cell to carry its normal cellular function, this was not the case in my analysis. Based on my findings, I would like to suggest that different regulatory mechanisms exist between the first and second round of endocycle in *Arabidopsis*.

I believe that a complete understanding of this difference in regulatory mechanism may be achieved by a high-throughput analysis of protein content and gene expression in 2C, 4C, and 8C endoreplicated cells. Identifying specific proteins and mRNA in endoreplicated nuclei will help better characterize the function of endoreplication. This could be achieved by further optimizing the conditions of protein and RNA extractions from sorted *Arabidopsis* nuclei yielding higher starting material of protein and RNA to carry on the iTRAQ and microarray analysis, respectively.

CHAPTER 3 LOCALIZATION AND SELF-INTERACTION OF *ARABIDOPSIS* TOPOISOMERASE VIB

3.1 Introduction

Topoisomerases are enzymes that are required to change the topology of DNA in crucial processes in prokaryotes and eukaryotes by relieving DNA torsional stress as a result of unwinding the DNA during transcription and replication⁴⁸. Topoisomerases are subdivided into two functional families; type I and type II.

Type I topoisomerases function as monomer enzymes that change the topology of the DNA by introducing a single strand break in their target DNA. They are subdivided into type IA and type IB according to which end of the DNA they link to; 5' for type IA, and 3' for type IB⁴⁸.

Type II topoisomerase are structurally and functionally different from type I topoisomerases. Unlike type I topoisomerase, a pair of strands in a DNA double helix are transiently broken in concert with dimerized type II topoisomerase, forming double staggered cuts on their target DNA by a phosphodiester bond linkage of its tyrosine to the DNA phosphate group. Unlike type I topoisomerase they are Mg⁺² and ATP-dependent. Similar to type IB, they relax negatively (subtractive helical twisting) and positively (additive helical twisting) supercoiled DNA. They are subdivided into type IIA and type IIB.

Eukaryotic TopIIA enzymes exist as dimers and form a 4bp staggered cut on their target DNA. They have been reported to play a role in the unknotting and decatenation of daughter chromosomes after the S-phase⁴⁹. Xie et al. reported the low detection of *Arabidopsis* TopIIA (AtTopIIA) polypeptide in mature seeds and vegetative tissues of *Arabidopsis*, and its rapid increase after germination and during the early phase of seedling development. These findings indicate the positive correlation between TopIIA expression and proliferation in *Arabidopsis*

thaliana, confirming the importance of this enzyme in chromosome condensation during mitotic cell cycle⁵⁰.

On the other hand, type IIB enzymes have been found in archaeobacteria and eukaryotes⁴⁸. Unlike type TopIIA, the enzyme results in a 2bp staggered cut at its target DNA. The enzyme is composed by heterotetramers of an A-subunit dimer (known as TopVIA) and a B-subunit dimer (known as TopVIB). Extensive structural studies have been conducted on TopVI *Sulfolobus shibatae* and *Methanosarcina mazei* (archaea). TopVIA (subunit A of TopIIB) shares the same TOPRIM (topoisomerase-primase) domain and catabolite activator protein (CAP) domain found in type TopIIA. Meanwhile, the TopVIB (subunit B of TopIIB) has a conserved ATPase domain and a transducer domain that is also found in type TopIIA. The transducer domain is thought to communicate the ATP state of the ATPase domain to the rest of the protein⁴⁸. Archaeal TopVIB also has two extra domains, one of which lies between the ATPase and transducer domain and contains a helix two turn helix (H2TH) conserved motif (Fig. 7)^{48,49,50}. The second extra domain lies after the transducer domain at the C-terminal end notated as an extension of the C-terminal domain (ECD). The crystal structure of *M.mazei* presents the ECD as an extension of the TopVIB projecting to the outside of the protein⁵¹. Kevin et al. suggested that the ECD of archaea TopVIB may act as a substrate sensor to distinguish the activity with type TopIIA, yet the relative activity of *M.mazei* TopVIB lacking the ECD on different substrate was not affected⁵¹. Kevin et al also suggested that the similarity of the secondary structure between the TopVIB ECD in *M.mazei* and immunoglobulin molecules may suggest that the ECD plays a role in binding with other proteins, which may alternate the localization of the TopVIB to a sub-cellular region⁵¹. However, no reports to date have shown the role of the C-terminal of TopVIB in the localization of the protein.

Proposed ATPase–strand passage cycle of type TopIIB that is composed of TopVIA and TopVIB subunits

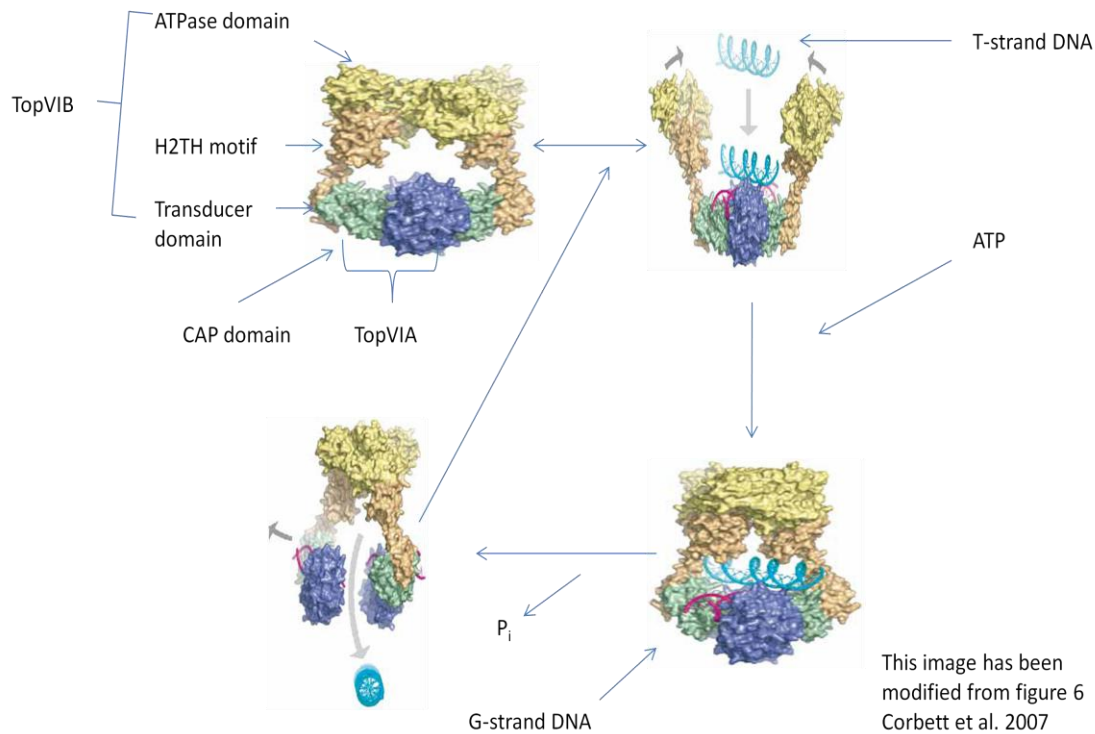


Figure 7. Type TopIIB working scheme showing the ATP possible structure along with the consequential changes after ATP binding. The TopVIB dimer of the type TopIIB enzyme can have more than one conformational structure before ATP binding, opened and closed. Upon the entry of the gate segment (G-strand) and the transfer segment (T-strand) DNA and ATP binding to the ATPase domain on TopVIB, the TopVIB subunit dimerizes and closes. This allows the TopVIA CAP domain to modify the topology of the G-strand DNA using its functional tyrosine group. This is followed by ATP hydrolysis and the passage of the T-strand through the cuts of the G-strand relieving the torsional stress. The hydrolysis of the second ATP molecule resets the enzyme to its old conformational state ready to modify the topology of the next stressed DNA. This image is modified from figure6 Berger et al.2007.

3.2 Cellular Effects in Mutations of the Topoisomerase VIB Gene in *Arabidopsis*

Plants carry TopVIB homologue as an exception among higher eukaryotes. Unlike AtTopIIA, no report to date has linked the functionality of *Arabidopsis* type TopIIB (AtTopVI) to the mitotic cell cycle. However, *Arabidopsis* TopVIB (AtTopVIB) subunit function has a link to endoreplication. Four mutants of TopVIB (*rhl3*, *hyp6*, *bin3*, and *TopVIB*) have been identified in *Arabidopsis thaliana* (AtTopVIB). The first AtTopVIB mutant, *rhl3* (root hairless mutant),

was identified during the ethyl-methylsulfonate (EMS) mutagenesis screening for plants that have fewer than normal root hairs. The mutant had an indistinguishable phenotype from *rhl2* that also shows a dwarf plant with only 10 hair projections per root⁵². An *rhl2* mutant leaf showed a reduction in the ploidy level (no more than 8C) compared to wildtype leaf (up to 32C). The second mutant, *hyp6* (hypocotyl mutants), was identified through EMS screening for plants that did not grow long hypocotyls in the dark. The mutant had a similar phenotype as *rhl2*, and the double mutant, *rhl2/hyp6*, was indistinguishable from either mutant.

Two *bin3* (brassinosteroid insensitive mutants) mutants were identified through the screening of plants that are insensitive to external application of brassinosteroid. *Bin3-1* was a T-DNA- knockout line, while *bin3-2* was an effect of EMS mutagenesis⁵³. One of the *bin3* mutants shows a dwarf plant with no reduction in the ploidy levels (up to 32C) compared to wild-type plant (up to 32C)⁵³.

Moreover, through the screening of T-DNA insertion libraries of the Arabidopsis knockout facility (Madison Wisconsin, USA), another AtTopVIB mutant was found. The mutant had dwarf plant with ploidy level reduction (no more than 8C). A comet assay, that involves lysing the nuclei under an electric current on agarose which allows DNA to travel according to the degree of DNA damage (the further distance the DNA travels the more nuclease degradation occurred), was done to evaluate the degree of chromosomal degradation. This T-DNA insertion mutant had a longer comet suggesting a more severe degradation by cellular nucleases compared to the wild-type due to the absence of the AtTopVIB functional activity⁵⁴.

3.3 Objectives

Objective I: Structural Comparison of TopVIB in Archaea and *Arabidopsis*

In order to understand the role of AtTopVIB in endoreplication and cell expansion at a

molecular and structural level, I examined the amino acid sequence of AtTopVIB using protein database (PDB) search engines, such as Pfam. I also compared the archaeal TopVIB crystal structure to AtTopVIB predicted structure based on the information in PDB servers, such as SwissProt⁵⁵. The first goal of this project was to identify unique domain(s) in plant TopVIB, which may contribute to the function of endoreplication.

Objective II: Localization and Interaction Analysis of TopVIB in Arabidopsis Protoplasts

I identified two unique domains in AtTopVIB that are conserved in rice TopVIB. I hypothesized that these domains function as a nuclear localization signal (NLS) that transports the AtTopVIB protein to the nucleus, or as interaction domains with other proteins. The second goal of this project was to test the hypothesis. In this thesis, I tested the localization and self-interaction of AtTopVIB by molecular imaging methods.

3.4 Materials and Methods

- **AtTopVIB Amplification from pDuet1 Vector**

The AtTopVIB clone was kindly provided by the Frank Hartung lab in a pDuet1 vector. TopVIB forward PCR primers were designed with an attB1.1 flanking sequence for the BP cloning reaction: (5'-GGGGACAAGTTTGTACAAAAAAGCAGGCTTTATGGCGGGTG-'3). The TopVIB reverse primer was designed to delete the stop codon out of the TopVIB sequence for protein expression and had an attB1.2 flanking sequence:

(5'-GGGGACCACTTTGTACAAGAAAGCTGGGTACAACATGAGCC-'3)

The pDuet1 containing the AtTopVIB was amplified using rTaq PCR kit (Takara Inc., Japan) with an annealing temperature of 60°C for 30 cycles in a 50 µL reaction mix. The 50 µL PCR product (amplicon) was run on 0.8% agarose gel.

- **DH5α Competent Cells Preparation**

A glycerol stock of DH5 α cells (Kristin Prufers LSU, USA) was spread over LB agar plate overnight at 37°C. A single colony was cultured in 4 mL LB broth for 16 hrs at 37°C with shaking. Two and a half milliliters of the culture was inoculated in 125 mL autoclaved SOB medium (20 g tryptone, 5 g yeast extract, and 0.5 g NaCl in 1 liter distilled water) in a 500 mL Erlenmeyer flask for 7 hrs at 37°C with shaking. Ten milliliters of the culture was inoculated in freshly autoclaved 125 mL SOB medium and incubated at 25°C with shaking for 9 hrs at 200 rpm. Optical density (O.D.) was measured at 600 nm, using SOB as a blank, until O.D. 0.55 was reached. At O.D. of 0.55, the remaining culture was divided into two 50 mL falcon tubes and centrifuged at 3000 rpm using a swing out rotor (Radius 28 mm) for 10 min at 4 °C. The supernatant was discarded and the pellet was re-suspended in 80 mL cold Inoue buffer (55 mM MnCl₂.4H₂O, 15 mM CaCl₂.2H₂O, 250 mM KCl, and 10 mM PIPES pH 6.7 in 1 liter of distilled water). The 80 mL suspension was centrifuged at 3000 rpm for 10 min at 4°C. The pellet was re-suspended in cold 20 mL Inoue buffer and 1.5 mL DMSO by swirling at 4°C. One and a half milliliter centrifuge tubes were chilled on ice and 200 μ L of competent cells were pipetted into each tube. Tubes were dropped in liquid nitrogen and stored at -80°C immediately.

DH5 α transformation efficiency was tested using 10 pg pUC19 plasmid (Invitrogen, USA). Fifty microliters of DH5 α competent cells were transfected with 1 μ L of pUC19 (10 pg/ μ L) heat shocked for 1 min followed by the addition of 150 μ L of SOB medium and incubation at 37°C for 30 min. The product was spread on an LB agar plate overnight at 37°C. Fifty colonies were counted on the plate which means that the transformation efficiency was 5 x 10⁶/ μ g of DNA.

- **Amplicon Insertion into Entry Clone**

The amplicon was excised from a 0.8% agarose gel and eluted using QIAEX II Gel Extraction Kit (Qiagen Sciences Maryland, USA). The eluted amplicon was quantified and 85 ng was mixed with 185 ng of pDNOR vector containing Zeocin as a selective marker using Gateway cloning BP clonase enzyme mix II (Invitrogen Inc., USA) in a total volume of 10 μ L and incubated at 25°C for 4 hours. The product, pENTRAtTopVIB, was used to transform 50 μ L of DH5 α competent cells and the transfected product was spread over LB agar containing Zeocin antibiotic (1 mg/mL) plate over night.

Three colonies were cultured in 3 mL of LB broth containing Zeocin (1 mg/mL). Plasmids were extracted using the mini-prep protocol adopted from the Molecular Cloning laboratory manual⁵⁶. The plasmid extracts from the three cultures were quantified using a nano-spectrophotometer and confirmed by digesting with *Bgl*III restriction enzyme. After confirming the digestion product of each plasmid, glycerol stocks of DH5 α cells were prepared in 40% glycerol and stored at -80°C.

Plasmid extracts were then sent for sequencing at Pennington sequencing facility (Baton Rouge, LA USA) using M13 forward and reverse primers. The pENTRTopVIB that did not undergo a mutation in its entire sequence was used beyond this point.

- **AtTopVIB LR reaction with pDuexAn1 and pDuexAc1.**

For the localization assay, a vector containing the yellow fluorescent protein (YFP) was used to clone YFP to the N-terminal end (pDuexAn1) or to the C-terminal (pDuexAc1)⁵⁷ end of pENTRAtTopVIB.3 using Gateway LR clonase mix II (Invitrogen Inc.). Both pDuexAn1 and pDuexAc1 vectors carry an Ampicillin resistance gene. One hundred and fifty nanograms of pENTRTopVIB.3 was mixed with 250 ng of pDuexAn1 and pDuexAc1 in a total volume of 10 μ L and incubated at 25 °C for 4 hrs. Fifty microliters of DH5 α was transformed with the An1 and

Ac1 vectors and spread over LB agar containing ampicillin (1 mg/mL) plates. Three colonies from each plate were cultured in LB broth containing ampicillin (1 mg/mL) and plasmids were extracted using the mini-prep and quantified as described previously. Once the plasmid construct was confirmed by restriction digestion using BglIII (BioRad, USA), plasmids were re-extracted using Plasmid Plus Midi-kit (Qiagen, USA). Plasmids were then quantified and used for the transformation of *Arabidopsis* protoplasts.

- **AtTopVIB LR reaction with pDuexAn6 and pDuexDn6**

For the split-luciferase assay, pENTRTopVIB.3 was cloned once into a vector containing the N-terminal fragment of luciferase [1-229aa (pDuexAn6)] and another containing the C-terminal of luciferase [230-311aa (pDuexDn6)]⁵⁷ using Gateway LR clonase mix II. Mini-preps and midi-preps were carried as described previously. Histone 2A tagged to the N-luc (pDuexAn6-H2A) and Histone 2B tagged to the C-luc (pDuexDn6-H2B)⁵⁷ were the positive control for the split-luciferase complementation assay.

- **Protoplast Preparation**

Arabidopsis thaliana plants of ecotype Columbia were grown in long day growth chamber (16 hrs of light and 8hrs of dark). One gram of 3 week old rosettes were gently cut using sharp scissors and sliced using a single razor blade into 1mm thin threads. Leaf threads were added to 10 mL digestion buffer (0.4 M mannitol, 20 mM MES pH5.7, 20 mM KCl, 10 mM CaCl₂) containing 0.1 g Cellulase and 0.025 g Macerozyme (Yakut Honsha Co. ltd. Tokyo, Japan) in a Petri dish. The plate was subjected to vacuuming for 30 min followed by incubation at 25°C in the dark for 9 hrs. The leaf suspension was then passed through a 100 µm cell strainer (BD Falcon, USA) and centrifuged at 100 x g for 3 min. The pellet was re-suspended in 10 mL of W5 buffer (154 mM NaCl, 125 mM CaCl₂, and 5 mM KCl, 2 mM MES pH 5.7) and

centrifuged at 100 x g for 3 min. The pellet was re-suspended in 10 mL W5 buffer and stored at 4°C for 30 min for the protoplast to settle down. The protoplast suspension was centrifuged again at 100 x g for 3 min and the pellet re-suspended in 10 mL of MMg buffer (0.4 M mannitol, 15 mM MgCl₂.6H₂O, and 4 mM MES pH 6.7 in 1 liter of distilled water). Protoplast suspension was centrifuged at 100 x g for 3 min and the pellet was re-suspended in 5 mL of MMg buffer. To calculate the concentration of the extracted protoplast, 40 µL of the protoplast solution was placed on a hemocytometer (Hausser Scientific Partnership, PA) under a light microscope at 40 X objective and the number of protoplast that falls in each 5sq. x 5sq. area was counted. The hemocytometer has 9 5sq x 5sq areas, so the average of the 9 areas was calculated.

- **Localization Assay**

For the localization assay, pDuexAn1RG, pDuexAn1TopVIB.3, and pDuexAc1TopVIB.3 plasmid concentrations were adjusted to 5 µg/µL. Five microliters of each plasmid were prepared in a total of 100 µL dH₂O for each separate experiment. A total of 80 µL was loaded in to 4 wells of a 96-well plate using a digital pipette (Fisherbrand Inc., USA) for each separate experiment. For the protoplast transfection, extracted protoplast concentration was adjusted to 2-3 x 10⁵ protoplast/mL. Transfection was started with the addition of 60 µL protoplasts followed by 40 µL PEG solution (40% v/v PEG4000 (Fluka 81240), 0.2 M mannitol, and 0.1 M CaCl₂) in to each well. The 96-well plate was immediately placed on an orbit shaker at 850 rpm for 15 seconds, and incubated at room temperature for 10 min. Two hundred microliters of WI buffer (0.5 M mannitol, 4 mM MES pH 5.7, and 20 mM KCl) was added to each well and the plate was centrifuged at 150 x g in a swing out rotor for 3 min. The supernatant was discarded by vacuum aspiration using a 96-well plate vacuum (BioTek, USA). This was followed by two additional WI buffer washes. After the last vacuum suction, the protoplast pellet

in each well was re-suspended in 200 μL of WI buffer and incubated in the dark at 25°C for 16 hrs. Twenty micro-liters of transfected protoplasts from each well bottom were stained with DAPI (10 $\mu\text{g}/\mu\text{L}$) and viewed under fluorescent microscope equipped with YFP and DAPI filters. Images of protoplasts showing DAPI staining and YFP localization were taken.

- **Self-interaction Assay (Split-luciferase Complementation Assay)**

For the split-luciferase assay, pDuexAn6TopVIB.3, pDuexDn6TopVIB.3, pDuexAn6H2A, and pDuexDn6H2B plasmid concentrations were adjusted to 500 ng/ μL . Five microliters of An6TopVIB.3 and Dn6TopVIB.3 plasmids were mixed in a total plasmid mix of 100 μL , prepared with dH₂O. Five micro liters of pDuexAn6H2A and pDuexDn6H2B plasmids were mixed in a total plasmid mix of 100 μL , prepared with dH₂O. pDuexAn1RG plasmid concentration was adjusted to 1 $\mu\text{g}/\mu\text{L}$. Five micro liters of pDuexAn1RG were mixed in a total plasmid mix of 100 μL , prepared with dH₂O. Each separate experiment was repeated 4 times by loading 80 μL of each plasmid mix to 4 wells on the 96-well plate, except for the mock wells that had no plasmid mix. The protoplast transfection procedure carried out is the same as the one used in the localization assay. ViviRen Live Cell substrate (Promega, USA), a luciferase substrate, was dissolved in DMSO at a concentration of 6mM and stored at -80°C. ViviRen solution was freshly diluted to 60 μM before use and 10 μl was added on to each well. The 96-well plate was placed on an orbit shaker at 850 rpm for 15 sec and luminescence was measured using Veritas microplate Luminometer (Turner Biosystems, USA).

3.5 Results

Structural Comparison of TopVIB in Archaea and *Arabidopsis*

Pfam⁵⁸ identified 2 independent uncharacterized domains. The first domain consists of 68 amino acids (aa) starting at position 86 aa (Fig. 8, 9). This domain lies within the ATPase

domain (45-234aa) towards the N-terminal end of AtTopVIB (Fig. 8). I designated this domain as IND (insertion of N-terminal domain). The second uncharacterized domain consists of 90aa starting at position 570aa. This domain lies right after the transducer domain (407-557aa) at the C-terminal end of AtTopVIB (Fig. 8, 10) as reported in archaeobacterial TopVIB. Comparison of amino acid sequence in *Arabidopsis*, *Oryza* (rice), and several archaeobacteria members that express the TopVIB protein, confirmed that the IND is well conserved between rice and *Arabidopsis* but missing in archaeobacterial members (Fig. 9).

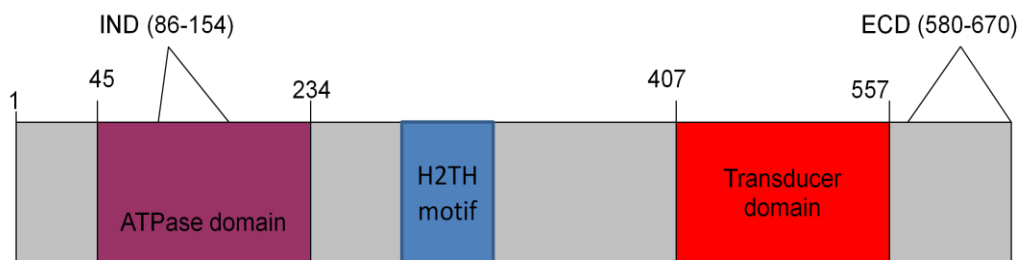


Figure 8. Schematic drawing of AtTopVIB showing its domains; ATPase domain, transducer domain, helix-2-turn-helix motif (H2TH) , insertion of the N-terminal domain (IND), and extension of the C-terminal domain (ECD). The numbers on top represents their amino acid positioning.

The second uncharacterized domain can be found only in species that express the TopIIA enzyme in their genome. The comparison of the amino acid sequence of the ECD among AtTopVIB (570-670aa), rice, and several members of the archaea TopVIB revealed that the ECD was not conserved between archaeobacteria and higher plants, but well conserved in *Arabidopsis* and rice (Fig.10).

Q9C5V6	FFAENKNIAGFDNPGKSLYTTVRELVENALDSAESISELPEVEVTIEEIVKSKFNSMIGI	92	TOP6B_ARATH
Q5ZPR4	FFAENKNIAGFDNPGKSLYTTMRELVENALDSAESISELPDIEIIIEEITKSKFNTMIGL	120	Q5ZPR4_ORYSI
O05207	FFKRNPELAGFPNPARALYQTVRELIENS LDATDVHGILPNIKITIDLIDDA-----	66	TOP6B_SULSH
Q972F0	FFKRNPELAGFPNPARALYQTVRELIENS LDATDVHGILPNIKITIDLIDES-----	66	TOP6B_SULSO
Q971T2	FFKRNPELAGFSPNPARALYQTVRELVENALDADVHNILPSIKIIIELVDPQ-----	65	TOP6B_SULTO
Q9YE64	FFAKNKELAGFANPTRALYQTIRELVENS LDATDAKGLPWIHISIRQIEGSEG-----	89	TOP6B_AERPE
Q8ZVM0	WFRNRRELAGFHNPTRALYQTIRELTENS LDATETYGILPTIYLRVNIIEDEQ-----	63	TOP6B_PYRAE
Q8PUB8	FFEKNRQILGFDSAPRSLITTVKEAVDNALDACEEAGILPDILVQVERTGPDY-----	73	TOP6B_METMA
Q8TQF7	FFEKNRQILGFDSAPRSLITTVKEAVDNALDACEEAGILPDILVQVERTGQDY-----	73	TOP6B_METAC
Q9HR31	FFEKNKHMLGFDSGARGLVTA VKEAVDNALDATEEAGILPDIYVEIS-EGRDY-----	82	TOP6B_HALSA
B0R4D3	FFEKNKHMLGFDSGARGLVTA VKEAVDNALDATEEAGILPDIYVEIS-EGRDY-----	82	TOP6B_HALS3
Q5V4R5	FFEKNKHMLGFDSPEARALVTA VKEAVDNALDACEEAGILPDIYVEIQ-ESGDY-----	81	TOP6B_HALMA
O29605	FFEKNKHILGYSNPAKALITTVKEAVDNALDACEEAGILPDIYFVRIS-KVDDH-----	64	TOP6B_ARCFU
Q58434	FFRKNKHMLGYSKIRSLTTIIHELVTNSLDACEEAGILPDIKVEIEKLGADH-----	73	TOP6B_METJA
O74020	FFRRNAAMLGYTGKIRSLTTIIHEAVTNSLDACEEAGILPTIRVEIEELGKEH-----	71	TOP6B_PYRHO
O27088	FFRKNKQMLGFTGKIRSLTIVFHELITNSPDAAEEAGILPEIKIDLKRIKGDH-----	73	TOP6B_METTH
	:* . * : * : . : : : : * * : : : . * * : : :		
Q9C5V6	IDRERVDTQLYDDYETEKARGKRLAKEARASEIQAKNLASGKKNKEPGVSKVLKARGEAS	152	TOP6B_ARATH
Q5ZPR4	VDRQRIDEELYDDPESAKAREKRLAKEARFPQETQAKNAALGKKVKEAPAARG-KGRGEAA	179	Q5ZPR4_ORYSI
O05207	-----RQ	68	TOP6B_SULSH
Q972F0	-----RQ	68	TOP6B_SULSO
Q971T2	-----KQ	67	TOP6B_SULTO
Q9YE64	-----RGGRP	94	TOP6B_AERPE
Q8ZVM0	-----KG	65	TOP6B_PYRAE
Q8PUB8	-----	73	TOP6B_METMA
Q8TQF7	-----	73	TOP6B_METAC
Q9HR31	-----	82	TOP6B_HALSA
B0R4D3	-----	82	TOP6B_HALS3
Q5V4R5	-----	81	TOP6B_HALMA
O29605	-----	64	TOP6B_ARCFU
Q58434	-----	73	TOP6B_METJA
O74020	-----	71	TOP6B_PYRHO
O27088	-----	73	TOP6B_METTH
Q9C5V6	YYKVTCKDNGKGMPHDDIPNMFGRVLSGTYG-LKQTRGKFGGLGAKMALIWSKMSTGLPI	211	TOP6B_ARATH
Q5ZPR4	FFGVTCCKDNGRGMPHDDIPNMLGRVLSGTYG-LRQTRGKFGGLGAKMALIWSKMSTGLPI	238	Q5ZPR4_ORYSI
O05207	IYKVNVDNGIGIIPPQEVNAPGRVLYSSKYV-NRQTRGMYGLGVKAAVLYSQMHQDKPI	127	TOP6B_SULSH
Q972F0	IYKVNVDNGIGIIPPQEVNAPGRVLYSSKYV-NRQTRGMYGLGVKAAVLYSQMHQDKPI	127	TOP6B_SULSO
Q971T2	IYKVNVDNGIGIIPPHIVNAPGKVLVYSSKYV-LRQTRGMYGLGVKAAVLYSQMYQERPV	126	TOP6B_SULTO
Q9YE64	RYTIVTVEDNGIGIVPVTSMAMAFGKVLVYSSKYV-IRQTRGMYGLGVKAAVLYSQMTAGTPV	153	TOP6B_AERPE
Q8ZVM0	WVSVYAEADNGIGIPGNEIPNVFGRVLYSSKYK-IKQHRGVFGLGLKMMVLYSQSTTNKPV	124	TOP6B_PYRAE
Q8PUB8	-VTVIIEDNGPGIVREQIPKVFYKLLYGSRFHALKQSRGQQGIGISAAVLYAQMTAGRHT	132	TOP6B_METMA
Q8TQF7	-VTVIIEDNGPGIVREQIPKVFYKLLYGSRFHALKQSRGQQGIGISAAVLYAQMTAGRHT	132	TOP6B_METAC
Q9HR31	-YTLIVEDNGPGITNAQIPKIFGKLLYGSRFHAREQSRGQQGIGISAAVLYSGLTSGRPV	141	TOP6B_HALSA
B0R4D3	-YTLIVEDNGPGITNAQIPKIFGKLLYGSRFHAREQSRGQQGIGISAAVLYSGLTSGRPV	141	TOP6B_HALS3
Q5V4R5	-YKLVVEDNGPGITKEQAPKIFGKLLYGSRFHAREQNRGQQGIGISAAVLYSGLTSGRPA	140	TOP6B_HALMA
O29605	-FKIVVEDNGPGIPREQIPKVFYKLLYGSRFHEIRQSRGQQGIGISAAVLYAQLTTGKPA	123	TOP6B_ARCFU
Q58434	-YKVAVEDNGPGIPLFIPKVFYKLLYGSRFHEIRQSRGQQGIGISAAVLYSGLTSGRPL	132	TOP6B_METJA
O74020	-YKVIIVEDNGPGIPEEYIPHVFGKMLAGTKAHRNIQSRGQQGIGISAAVLYAQLTTGKPT	130	TOP6B_PYRHO
O27088	-YILRHQDNGPGIPEKYIPKVFCTMFAGSKFR-NIQSRGQQGLGCSGCVLLSQMTTGKPV	131	TOP6B_METTH

Figure 9. N-terminal sequence alignment of AtTopVIB (red rectangle) in comparison with *Oryza* (rice, green rectangle) and different members of archaeobacteria. The labels on the left-hand side are accession numbers for the following organisms respectively; *Arabidopsis thaliana* (Q9C5V6), *Oryza sativa* (Q5ZPR4), *Sulfolobus shibatae* (O05207), *Sulfolobus solfataricus* (Q972F0), *Sulfolobus tokodaii* (Q971T2), *Aeropyrum pernix* (Q9YE64), *Pyrobaculum aerophilum* (Q8ZVM0), *Methanosarcina mazei* (Q8PUB8), *Methanosarcina acetivorans* (Q8TQF7), *Halobacterium salinarium* (B0R4D3), *Haloarcula marismortui* (Q5V4R5), *Archaeoglobus fulgidus* (O29605), *Pyrococcus furiosus* (Q8U0K8), *Methanocaldococcus jannaschii* (Q58434), *Pyrococcus horikoshii* (O74020), *Methanobacterium thermoautotrophicus* (O27088).

Q9C5V6	KKLQARERQDRKRNLNRYIPDVARAIMETLGEIADESPPKRPHYDKEDEELLEKVNSEEV	606	TOP6B_ARATH
Q5ZPR4	KKLQARERQDRKRNLNRYIPDVARAIMETLGEIADESPPKRPHYDKEDEELLEKVNSEEV	633	Q5ZPR4_ORYSI
O05207	EKRKEQEAKKKLLDAYLKYIPEVSRSLATFLASGNKEL---VSKYQNEISEGLFKLISKAL	513	TOP6B_SULSH
Q97ZF0	EKRKEQEAKKKLLDAYLKYIPEVSRSLAIFLASNKEL---VPKYQGEIVEGLFKLISKAL	513	TOP6B_SULSO
Q971T2	EKRKEEAAKRLITYLKYIPEVSRGLALFLVGGDKQK---IGDAYSDLREKLLKIALNKL	513	TOP6B_SULTO
Q9YE64	RKAREEEAIRRSVTLAKYIPEVAVSLAYFLRPPSKWQPP-KPEEVKKIQEALIKIVARHI	542	TOP6B_AERPE
Q8ZVM0	RKEKEMEMLNKYISLAKYVEEIAYNLSMITR-IEKES---LAKNLHTLIERKIGLTIEEL	506	TOP6B_PYRAE
Q8PUB8	KQSNLKKRREKEIIITKVLPKLAAKVAHVLEKDVDPINPVVAKIMGNLLVHRVIRKNGDG	524	TOP6B_METMA
Q8TQF7	KQSNLKKRREKEIIITKVLPKMAVKVANILEKDVDPINPVVAKIMGNLLVYRKKVKSNGDG	524	TOP6B_METAC
Q9HR31	KRQSMRKRQKQDVIMDILPTMAEKVGLTGRGGVDVSDSLARIMNNVLERARSDDGQ-	717	TOP6B_HALSA
B0R4D3	KRQSMRKRQKQDVIMDILPTMAEKVGLTGRGGVDVSDSLARIMNNVLERARSDDGQ-	717	TOP6B_HALS3
Q5V4R5	KRRSMQQRREKQDKLATILPEMAEKLETEVDNDELHIDDSLARIMNNVLEREVEDD---	713	TOP6B_HALMA
O29605	RKSRQKQKKKKEEMIGKVLPLIAKKVCEILEKEPLEIDRIVARIMGYLHVERIVEERDG-	513	TOP6B_ARCFU
Q58434	RIRREAEERKRRKVMKYARIFAELANILNKPVDEIEEKVVKLE-----	660	TOP6B_METJA
O74020	GKYRMYQIKRRKTLKYLPEIARSLHILTGEPEEKIREYFLKLIESKIEVEEVESVEVE	560	TOP6B_PYRHO
O27088	KKKAKEEAQRAKIFESYVVIKQAALLAEREPEPYRELLDVTTR-RAKLEILGGITE-	523	TOP6B_METTH
:			
Q9C5V6	TKETLKEKLAEHVEQVDYEMALEYATQSGVSEEPRENIYLQHLDPNKSNFIDLHSPFTVF	666	TOP6B_ARATH
Q5ZPR4	TEMTFRDCLTQHVEQVDYEMALEYAMQSGVSEEPREALYLNLSLEG-SYKFIQSPVVFV	692	Q5ZPR4_ORYSI
O05207	DLIN----IEEYRKVYR--VDSE-----	530	TOP6B_SULSH
Q97ZF0	DLIN----IEEYRKVYK--VDSE-----	530	TOP6B_SULSO
Q971T2	EVNDKK--LEEEIRNYK--VEEL-----	532	TOP6B_SULTO
Q9YE64	ELPPVDGKTEDPEAIVRRIVESVELE-----	568	TOP6B_AERPE
Q8ZVM0	VKHT----LSMSSTSQEVEVATPQ-----	527	TOP6B_PYRAE
Q8PUB8	TVDVAIRVKNFGTSAYSFRVHEMLPCKVSGARPEPRVVTMGNDYDYVWDISASAGSSKVL	584	TOP6B_METMA
Q8TQF7	TADVAIRVKNFGTSAHVHEMLPCKINGARPEPRVVTMDNDYDYVWDVSAAGSSKVL	584	TOP6B_METAC
Q9HR31	--TVTTLRVENHGTGSVDVVDIVSAEPDGVGDDASVVMDDDEYFVKWTPAVAGDDAAEL	775	TOP6B_HALSA
B0R4D3	--TVTTLRVENHGTGSVDVVDIVSAEPDGVGDDASVVMDDDEYFVKWTPAVAGDDAAEL	775	TOP6B_HALS3
Q5V4R5	--TVRVRINDDTNADVELTDIVTAEP-QVTNGATVVEMDGEWFKWSPTVAGGETAVL	770	TOP6B_HALMA
O29605	VKVVTIRVSNFTRSKKSIKLYEMCSG---NVEADGAKVSGSGYSTVTVWSLEVKPDEEVEV	570	TOP6B_ARCFU
Q58434	-----	660	TOP6B_METJA
O74020	EAEA-----	564	TOP6B_PYRHO
O27088	-----	523	TOP6B_METTH
:			
Q9C5V6	RLML-----	671	TOP6B_ARATH
Q5ZPR4	REIP-----	697	Q5ZPR4_ORYSI
O05207	-----	531	TOP6B_SULSH
Q97ZF0	-----	531	TOP6B_SULSO
Q971T2	-----	533	TOP6B_SULTO
Q9YE64	-----	569	TOP6B_AERPE
Q8ZVM0	-----	528	TOP6B_PYRAE
Q8PUB8	SYKIESASEEELQKLPQLIVEGIEEELVTGAKAFRGV	621	TOP6B_METMA
Q8TQF7	SYKIESATVEELRKLPLIVEGIEEELVTGAKAFRGV	621	TOP6B_METAC
Q9HR31	TYSVDADADCELS-----VSGVADARLTVSEADT--	805	TOP6B_HALSA
B0R4D3	TYSVDADADCELS-----VSGVADARLTVSEADT--	805	TOP6B_HALS3
Q5V4R5	EYSVTDEAEFTVS-----VDGIEEEKLTVNA----	797	TOP6B_HALMA
O29605	SYRLKGRINKNP-----LVEGV EEDLLSGAEVMNFA	602	TOP6B_ARCFU
Q58434	-----	661	TOP6B_METJA
O74020	-----	565	TOP6B_PYRHO
O27088	-----	524	TOP6B_METTH

Figure 10. C-terminal sequence alignment of AtTopVIB (red rectangle) in comparison with *Oryza* (rice, green rectangle) and different members of archaeobacteria. The labels on the left-hand side are accession numbers for the following organisms respectively; *Arabidopsis thaliana* (Q9C5V6), *Oryza sativa* (Q5ZPR4), *Sulfolobus shibatae* (O05207), *Sulfolobus solfataricus* (Q97ZF0), *Sulfolobus tokodaii* (Q971T2), *Aeropyrum pernix* (Q9YE64), *Pyrobaculum aerophilum* (Q8ZVM0), *Methanosarcina mazei* (Q8PUB8), *Methanosarcina acetivorans* (Q8TQF7), *Halobacterium salinarium* (B0R4D3), *Haloarcula marismortui* (Q5V4R5), *Archaeoglobus fulgidus* (O29605), *Pyrococcus furiosus* (Q8U0K8), *Methanocaldococcus jannaschii* (Q58434), *Pyrococcus horikoshii* (O74020), *Methanobacterium thermoautotrophicus* (O27088).

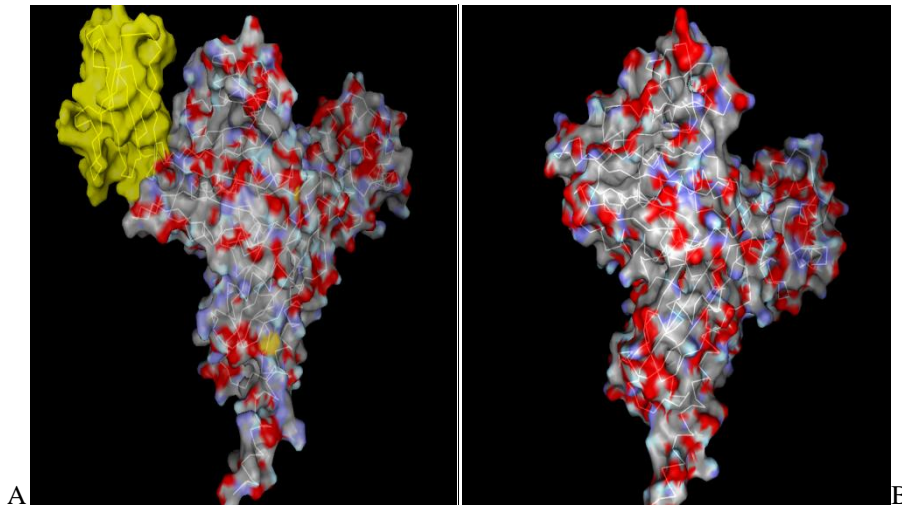


Figure 11. A) The AtTopVIB N-terminal surface density predicted structure using the protein database (PDB) software with the insertion in the N-terminal domain (IND) in yellow. B) *S.shibatae* TopVIB N-terminal crystallized structure missing the IND.

The SwissProt protein server was then used to predict the structure of the IND of AtTopVIB⁵⁵. This server uses the amino acid sequence of AtTopVIB and search for a homology in proteins with known crystal structure (personal communication, Blake Crochet). If it fails to match the amino acid sequence, it predicts the secondary structure of the protein using the structural dynamics of amino acids found in its database (personal communication, Blake Crochet). The predicted structure of AtTopVIB was almost similar to the crystal structure of *M.mazei* TopVIB structure except for the IND, which formed a “bubble” like extension at the ATPase domain in AtTopVIB (Fig. 11).

Construction of Plasmid Vectors for Molecular Imaging Assay

The AtTopVIB clone was kindly provided in a pDuet1 vector by the Frank Hartung lab. In order to utilize the AtTopVIB clone in the localization and interaction assay, I amplified the AtTopVIB clone and inserted the amplicon into gateway cloning pDONR vector. This was done using a Gateway BP clonase reaction producing a pENTRAAtTopVIB. Three pENTRAAtTopVIB clones were cultured and digested to confirm that they were the right constructs. The resulting

plasmid, pENTRAtTopVIB.3, that does not undergo any point-mutation compared to the original AtTopVIB sequence was used for further cloning. Using Gateway cloning, AtTopVIB from the pENTRTopVIB plasmid was cloned into plasmids carrying YFP. Plasmids carrying the YFP on the N-terminal of AtTopVIB (pDuexAn1-AtTopVIB), YFP on the C-terminal of AtTopVIB (pDuexAc1-AtTopVIB), or as a control, YFP on the N-terminal of full-length luciferase (pDuexAn1RG), were used for the localization assay (Fig.12).

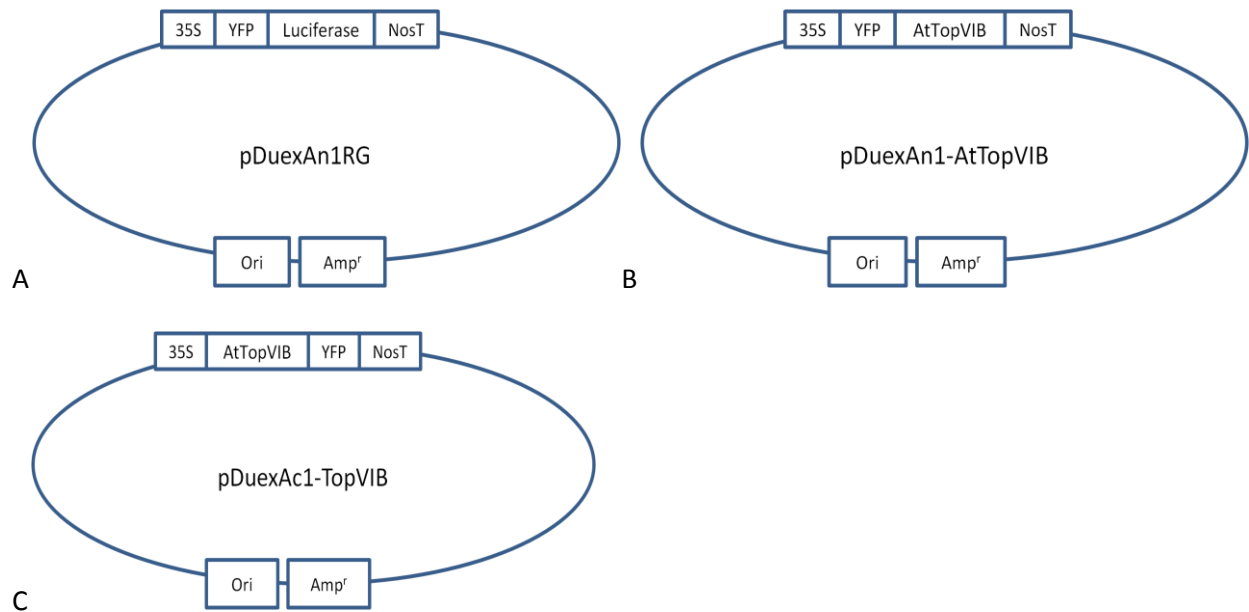


Figure 12. Schematic drawing of pDuex vectors used in the localization assay. A) pDuexAn1RG vector carrying a 35S; cauliflower mosaic virus 35S promoter, YFP; yellow fluorescent protein clone, Luciferase; full-length luciferase clone, NosT; nopaline synthase terminator, Ori; the origin of replication and Amp^R; ampicillin resistance gene. B) pDuexAn1-AtTopVIB vector carrying a 35S promoter, YFP tagged to the N-terminal end of AtTopVIB; full-length AtTopVIB clone, NosT terminator, Ori, and Amp^R. C) pDuexAc1-TopVIB vector carrying a 35S promoter, YFP tagged to the C-terminal of AtTopVIB, NosT terminator, Ori, and Amp^R.

For the AtTopVIB self-interaction assay, Gateway cloning was used to clone AtTopVIB from the pENTRAtTopVIB plasmid into plasmids carrying the N-terminal fragment of luciferase (pDuexAn6-AtTopVIB), the C-terminal fragment of luciferase (pDuexDn6-AtTopVIB). As a control for the self-interaction assay, the N-terminal fragment of luciferase was cloned to the N-

terminal of histone 2A (pDuexAn6-H2A) and the C-terminal fragment of luciferase was cloned to the N-terminal of Histone 2B (pDuexDn6-H2B) (Fig.13).

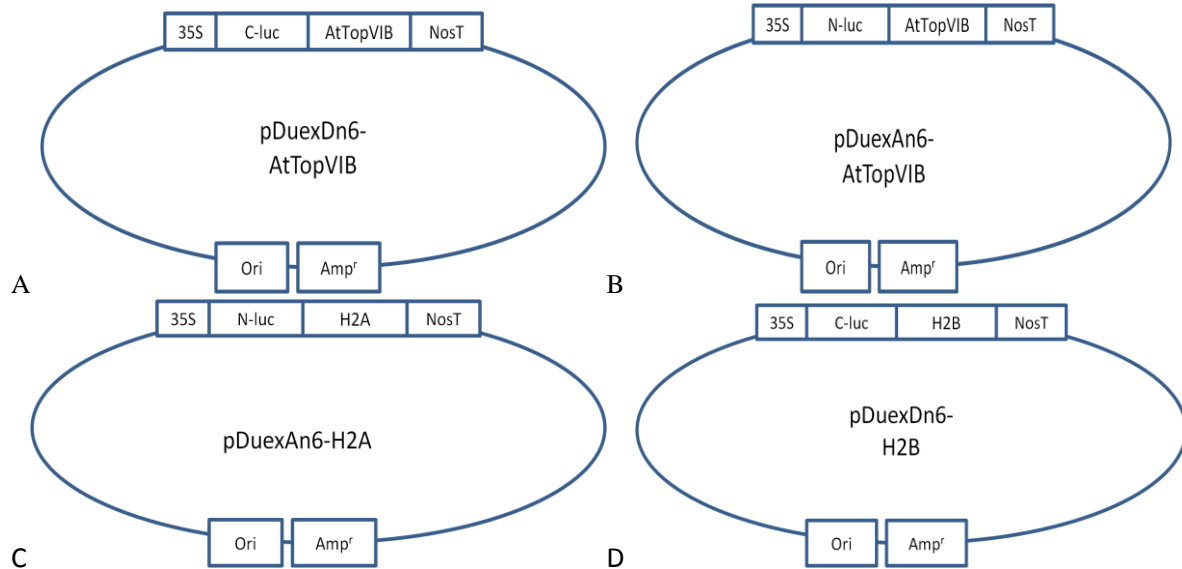


Figure 13. Schematic drawing of pDuex vectors used in the self-interaction assay (split-luciferase complementation assay). A) pDuexDn6-AtTopVIB vector carrying a 35S; cauliflower mosaic virus 35S promoter, C-luc; C-terminal fragment of *Renilla* luciferase, AtTopVIB; full-length AtTopVIB clone, and NosT; nopaline synthase terminator, Ori; the origin of replication and Amp^R; ampicillin resistance gene. B) pDuexAn6-TopVIB vector carrying a 35S promoter, N-luc; N-terminal fragment of *Renilla* luciferase, AtTopVIB clone, NosT terminator, Ori, and Amp^R. C) pDuexAn6-H2A vector carrying a 35S promoter, N-luc, H2A; full-length histone 2A clone, NosT terminator, Ori, and Amp^R. D) pDuexDn6-H2B vector carrying a 35S promoter, C-luc, H2B; full-length histone 2B clone, NosT terminator, Ori, and Amp^R.

Localization Assay

To test the cellular localization of the AtTopVIB, *Arabidopsis* protoplasts were transformed with plasmids expressing full-length luciferase tagged with YFP (pDuexAn1RG), or AtTopVIB tagged with YFP at the N-terminal (pDuexAn1-AtTopVIB), or AtTopVIB tagged with YFP at the C-terminal (pDuexAc1-AtTopVIB) (Fig. 12). YFP localization in protoplasts was determined using fluorescence microscopy equipped with a YFP filter. Protoplasts were stained with DAPI to identify nuclei. Protoplasts transformed with pDuexAn1RG were first observed with microscope equipped with DAPI and YFP filters. The images clearly showed the localization of the luciferase protein tagged with YFP in the cytosol and nucleus indicating no

specific cellular localization of the luciferase protein (Fig. 14). Protoplasts transformed with pDuexAn1-AtTopVIB were then observed under DAPI and YFP filters. Localization of the pDuexAn1-AtTopVIB strictly to the nucleus of the protoplast indicated the specific localization of AtTopVIB protein to the nucleus (Fig. 15). I was unable to identify YFP localization in protoplasts transformed with pDuexAc1-AtTopVIB. A control protoplast in which plasmid pDuexAc1-H2B, expressing histone 2B with YFP at its C-terminal was transformed, exhibited expression of the fusion protein (data not shown). This suggested that expression of TopVIB-YFP may have problems in its translation or at the post translational level.

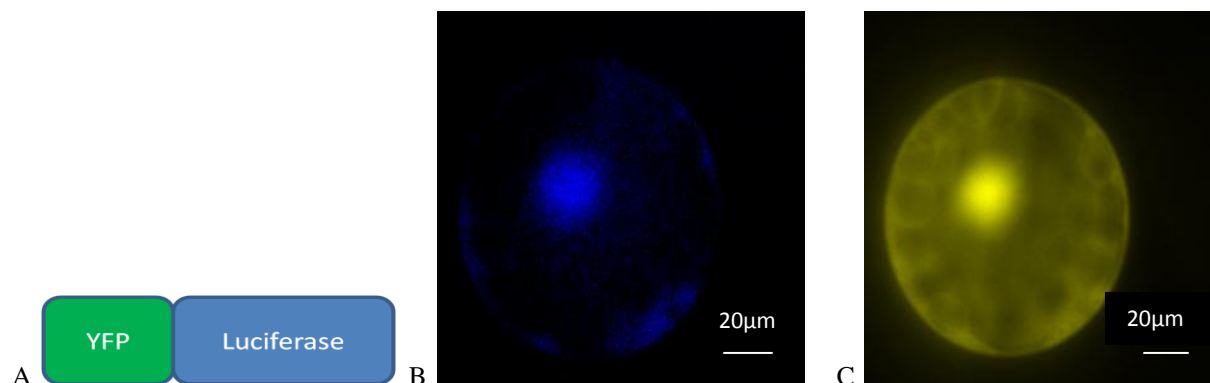


Figure 14. A) Schematic drawing of An1RG showing the YFP tagged to the N-terminal of luciferase clone. Deconvoluted images of *Arabidopsis thaliana* protoplast transformed with pDuexAn1RG. B) Transformed protoplast stained with DAPI showing the localization of the DAPI in the nucleus. C) Transformed protoplast showing the localization of YFP-luciferase in cytoplasm and the nucleus.

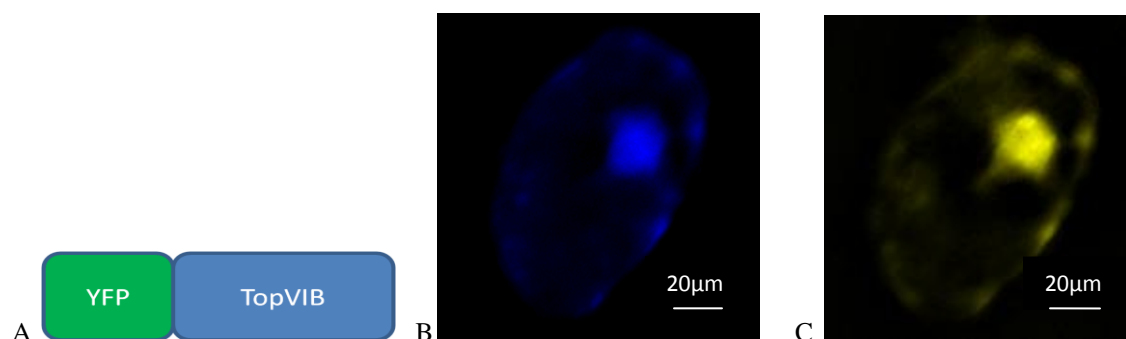


Figure 15. A) Schematic drawing of An1-AtTopVIB showing the YFP tagged to the N-terminal of AtTopVIB clone. Deconvoluted images of *Arabidopsis thaliana* protoplast transformed with pDuexAn1-AtTopVIB. B) Transformed protoplast stained with DAPI showing the localization of DAPI to the nucleus. C) Transformed protoplast showing a clear localization of YFP-AtTopVIB in the nucleus.

Split-luciferase Complementation Assay

To test the AtTopVIB self-interaction, protoplasts were transformed with pDuexAn6-AtTopVIB and pDuexDn6-AtTopVIB. Histone 2A and histone 2B were used as a control⁵⁷. The split-luciferase complementation assay was used to detect protein- protein interaction in an organism of interest⁵⁷. In this assay, protein-protein interaction between the bait and prey protein, fused to the N-terminal and C-terminal fragments of luciferase, complement the luciferase activity. The average of 4 independent transformations for each experiment was compared in this study (Fig. 16).

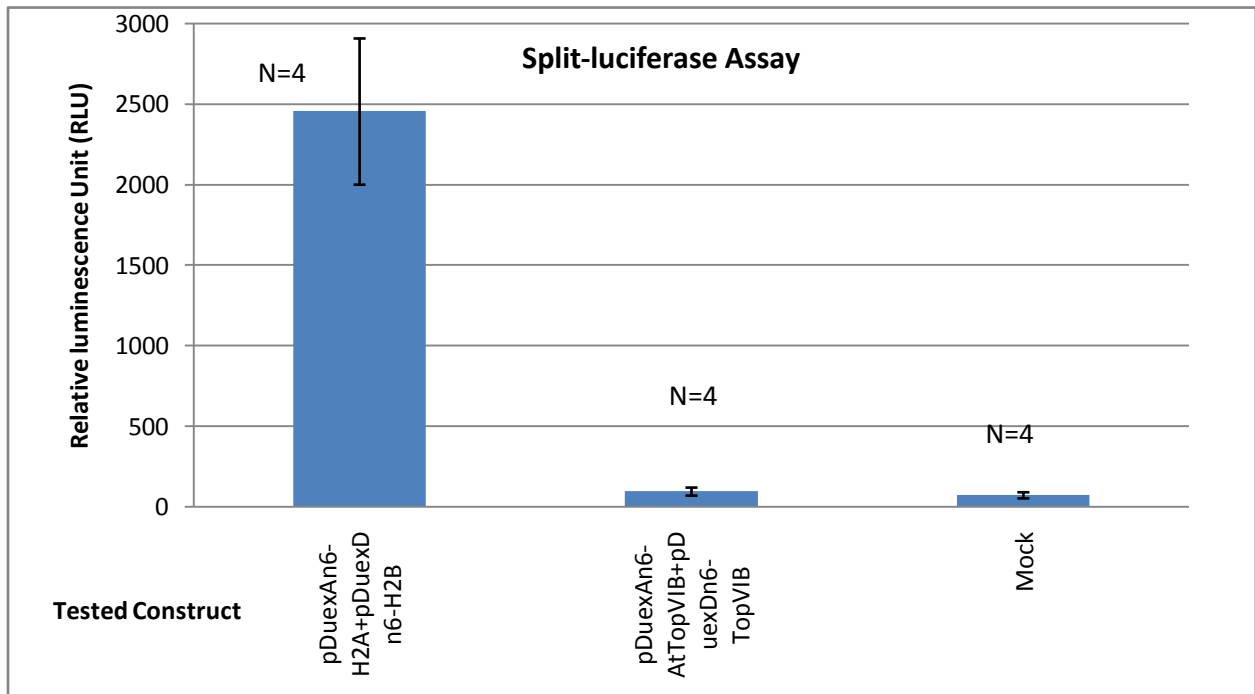


Figure 16. The average of relative luminescence unit in *Arabidopsis* protoplast transformed with pDuexAn6-H2A and pDuexDn6-H2B, or pDuex An6-AtTopVIB and pDuexDn6-AtTopVIB, or no DNA sample (Mock). (N is the number of independent transformation for each experiment)

The protoplast transformed with pDuexAn6-TopVIB and pDuexDn6-TopVIB constructs showed low luminescence, almost as the mock protoplasts. While the protoplasts transformed with pDuexAn6-H2A and pDuexDn6-H2B constructs showed significantly high luminescence.

This low luminescence production indicates no complementation of the split luciferase tags due to the absence of AtTopVIB self interaction.

3.6 Discussion

The results of my amino acid homology search and structural prediction of AtTopVIB identified two novel uncharacterized domains, the insertion in the N-terminal domain (IND) and the extension in the C-terminal domain (ECD). Using particle bombardment transformation, it has been shown that the N-terminal end (1-144 aa) of AtTopVIB tagged with green fluorescent protein (GFP-AtTopVIB₁₋₁₄₄) is localized to the nucleus in *Arabidopsis* seedlings⁵⁴. Together with my analysis, I suggest that the IND (86-154aa) may encode the NLS.

Shirasu et al. reported that AtTopVIB self-interacts in a yeast two-hybrid assay (Y2H)³³. However, my split-luciferase complementation assay results indicated that AtTopVIB interaction was very weak, if it occurs, in *Arabidopsis* protoplasts. One explanation for this weak interaction is the incorrect fusion of the split luciferase tags. In order for the luciferase enzyme to become active, the N-terminal and the C-terminal fragments of split-luciferase protein have to be properly oriented. In my control experience, the N-terminal and C-terminal luciferase fragments were fused to the N-terminal end of H2A and H2B, respectively, and showed a significantly high luminescence. Therefore, the low interaction of AtTopVIB using the split-luciferase assay may be due to the artifact of the assay.

Another explanation is that other protein(s) in *Arabidopsis* protoplasts may bind to the ECD region of the TopVIB protein, resulting in a low self-interaction of AtTopVIB. TopVIB has been reported to interact with the TopVIA dimer and with itself⁵⁴. In *M.mazei*, the self-interaction of TopVIB occurs in Y2H only in the presence of ATP⁵⁴. I suggest that the ECD region may work as a “guard” that has a role in binding another protein blocking the self-

interaction prior to ATP binding. Because a Y2H does not contain the *Arabidopsis* proteins that may inhibit the AtTopVIB interaction, the data may not agree with my split-luciferase data. However, I was unable to test the TopVIB interaction with the deleted ECD region using the split-luciferase complementation assay because of time constraint.

In conclusion, I found the localization of TopVIB to the nucleus in *Arabidopsis thaliana* using a YFP tagging system. The split-luciferase complementation assay suggests that there is an insignificant self-interaction of AtTopVIB in a plant system. This may owe either to the artifact of the split-luciferase complementation assay or to a possibility that other protein(s) are involved in binding to the ECD region of AtTopVIB preventing self-interaction prior ATP binding. This study has set the stage for my next goal: to carry the same assays using AtTopVIB with deleted ECD or IND. This should better characterize the functionality of ECD and IND in the localization and dimerization of TopVIB in higher plants.

REFERENCES

- ¹ Dennis Francis (2007) The plant cell cycle-15 years on. *New Phytologist*. **174**:261-278.
- ² Véronique Boudolf, Stephane Rombauts, Mirande Naudts, Dirk Inzé and Lieven De Veylder (2001) Identification of novel cyclin-dependent kinases interacting with CKS1 protein of *Arabidopsis*. *Experimental Botany*, **52**:341-50.
- ³ Joubes J, Chevalier C. (2000) Endoreplication in higher plants. *Plant Molecular Biology* **43**:735-45.
- ⁴ W. Dewitte and J. Murray (2005) The Plant Cell Cycle. *Plant Biology*. **54**:235-64.
- ⁵ Fausto, N. and Campbell, J. N. (2003) The role of hepatocytes and oval cells in liver regeneration and repopulation. *Mechanisms of Development*, **120**:117-130.
- ⁶ Sarah P Otto and Jeannette Whitton (2000) Polyploidy incidence and evolution. *Annual Review of Genetics*, **34**: 401-437.
- ⁷ Matthew J. Hegarty and Simon J. Hiscock (2008) Genomic Clues to the evolutionary success of Polyploidy plants. *Current Biology* **18**:435-44.
- ⁸ Zuzana Storchova and Christian Kuffer (2008) The consequences of tetraploidy and aneuploidy. *Journal of Cell Science*, **121**:3859-66.
- ⁹ Katya Ravid , Jun Lu, Jeffrey M. Zimmet, Matthew R. Jones (2002) Roads to Polyploidy: The Megakaryocyte Example. *Journal of Cellular Physiology*, **190**:7-20.
- ¹⁰ A. M. Gladwin and J. F. Martin (1990) The control of megakaryocyte ploidy and platelet production: biology and pathology. *International Journal of Cell Cloning*, **8**: 291-298.
- ¹¹ Amy E. Geddis, Kenneth Kaushansky (2006) Endomitotic megakaryocytes form a midzone in anaphase but have a deficiency in cleavage furrow formation. *Cell Cycle*, **5**:538:45.
- ¹² Zhimulev IF, Belyaeva ES, Semeshin VF, Koryakov DE, Demakov SA, Demakova OV, Pokholkova G. V., Andreyeva E. N. (2004) Polytene Chromosomes: 70 Years of Genetic Research. *International Review of Cytology*, **241**:203-75.
- ¹³ Ashburner M. (1990) Puffs, genes, and hormones revisited. *Cell* **61**:1-3.
- ¹⁴ Sugimoto-Shirasu, K. and Roberts K. (2003) "Big it up": endoreduplication and cell-size control in plants. *Current Opinion in Plant Biology*, **6**:544-53.

- ¹⁵ Thomas J. Leach, Heather L. Chotkowski, Michael G. Wotring, Robert L. Dilwith, and Robert L. Glaser (2000) Replication of Heterochromatin and Structure of Polytene Chromosome. *Molecular and Cellular Biology*, **20**:6308-6316.
- ¹⁶ Lilly MA and Spradling AC. (1996) The *Drosophila* endocycle is controlled by Cyclin E and lacks a checkpoint ensuring S-phase completion. *Genes Deviation*, **10**:2514–2526.
- ¹⁷ R. J. Duronio, P. C. Bonnette and P. H. O'Farrell (1998) Mutations of the *Drosophila* *dDP*, *dE2F*, and *cyclin E* Genes Reveal Distinct Roles for the E2F-DP Transcription Factor and Cyclin E during the G1-S Transition. *Molecular and Cellular Biology*, **18**:141-51.
- ¹⁸ I. Royzman (1998) S phase and differential DNA replication during *Drosophila* oogenesis. *Genes to Cells*, **3**:767-776.
- ¹⁹ Leach T. J., Chotkowski H. L., Wotring M. G., Dilwith R. L. and Glaser R. L. (2000) Replication of Heterochromatin and Structure of Polytene Chromosomes. *Molecular and Cellular Biology*, **20**:6308–6316.
- ²⁰ Zuzana Storchova and David Pellman (2004) From Polyploidy to Aneuploidy, Genome Instability and Cancer. *Nature Reviews Molecular Cell Biology*, **5**:45-54.
- ²¹ J. E. Melaragno, B. Mehrotra and A. W. Coleman (1993) Relationship between endopolyploidy and cell size in epidermal tissue of *Arabidopsis*. *Plant cell*, **5**:1661-1668.
- ²² Véronique Boudolf, Kobe Vlieghe, Gerrit T.S. Beemster, Zoltan Magyar, Juan Antonio Torres Acosta, Sara Maes, Els Van Der Schueren, Dirk Inzé and Lieven De Veylder (2004). The plant-specific cyclin-dependent kinase CDKB1;1 and transcription factor E2FA-DPa control the balance of mitotically dividing and endoreplicating cells in *Arabidopsis*. *Plant Cell*, **16**:2683-92.
- ²³ Arp Schnittger, Ulrike Schöbinger, York-Dieter Stierhof and Martin Hülskamp (2002) Ectopic B-type cyclin expression induces mitotic cycles in endoreplicating *Arabidopsis* trichomes. *Current Biology*, **12**:415-20.
- ²⁴ Fulop K, Tarayre S, Kelemen Z, Horvath G, Kevei Z, Nikovics K, Bakó L, Brown S, Kondorosi A, Kondorosi E (2005) *Arabidopsis* anaphase-promoting complexes: multiple activators and wide range of substrates might keep APC perpetually busy. *Cell Cycle*, **4**:1084-92.
- ²⁵ Jose Maria Vinardell, Elena Fedorova, Angel Cebolla, Zoltan Kevei, Gabor Horvath, Zoltan Kelemen, Sylvie Tarayre, François Roudier, Peter Mergaert, Adam Kondorosi and Eva Kondorosi (2003) Endoreduplication Mediated by the Anaphase-Promoting Complex Activator CCS52A Is Required for Symbiotic Cell Differentiation in *Medicago truncatula* Nodules. *The Plant Cell*, **15**:2093-105.
- ²⁶ Zachary Larson-Rabin, Ziyu Li, Patrick H. Masson, and Christopher D. Day (2009) FZR2/CCS52A1 Expression Is a Determinant of Endoreduplication and Cell Expansion in *Arabidopsis*. *Plant Physiology*, **149**:874-84.

- ²⁷ Michelle L. Churchman, Matthew L. Brown, Naohiro Kato, Viktor Kirik, Martin Hülskamp, Dirk Inzé, Lieven De Veylder, Jason D. Walker, Zhengui Zheng, David G. Oppenheimer, Taylor Gwin, Jason Churchman and John C. Larkin (2006) SIAMESE, a Plant-Specific Cell Cycle Regulator, Controls Endoreplication Onset in *Arabidopsis thaliana*. *The Plant Cell*, **18**:3145-3157.
- ²⁸ Keiko Sugimoto-Shirasu, Nicola J Stacey, Julia Corsar, Keith Roberts and Maureen C McCann (2002) DNA Topoisomerase VI Is Essential for Endoreduplication in *Arabidopsis*. *Current Biology*, **12**:1782-86.
- ²⁹ Kato, N. and Lam, E. (2003) Chromatin of endoreplicated pavement cells has greater range of movement than that of diploid guard cells in *Arabidopsis thaliana*. *Journal of Cell Science*, **116**:2195-201.
- ³⁰ Reynold I. Lopez-Soler, Robert D. Moir, Timothy P. Spann, Reimer Stick and Robert D. Goldman (2001) A role for nuclear lamins in nuclear envelope assembly. *Journal of Cell Biology*, **154**: 61-70.
- ³¹ Patricia A. Harder, Rebecca A. Silverstein, and Iris Meier (2000) Conservation of Matrix Attachment Region-Binding Filament-Like Protein 1 among Higher Plants. *Plant Physiology*, **122**:225-32.
- ³² Christian Breuer, Nicola J. Stacey, Christopher E. West, Yunde Zhao, Joanne Chory, Hirokazu Tsukaya, Yoshitaka Azumi, Anthony Maxwell, Keith Roberts and Keiko Sugimoto-Shirasu (2007) BIN4, a Novel Component of the Plant DNA Topoisomerase VI complex, is Required for Endoreplication in *Arabidopsis*. *The plant Cell*, **19**:3655-68.
- ³³ Keiko Sugimoto-Shirasu, Gethin R. Roberts, Nicola J. Stacey, Maureen C. McCann, Anthony Maxwell, and Keith Roberts (2005) RHL1 is an essential component of the plant DNA topoisomerase VI complex and is required for ploidy-dependent cell growth. *Plant Biology*, **51**:18736-741.
- ³⁴ Viktor Kirik, Andrea Schrader, Joachim F. Uhrig and Martin Hülskamp (2007) MIDGET unravels functions of the *Arabidopsis* topoisomerase VI complex in DNA endoreplication, Chromatin condensation, and transcriptional silencing. *The Plant Cell*, **19**:3100-10.
- ³⁵ Jianlin Wang, Lu Tian, Andreas Madlung Hyeon-Se Lee, Meng Chen, Jinsuk J. Lee, Brian Watson, Trevor Kagochi, Luca Comai and Z. Jeffrey Chen (2004) Stochastic and Epigenetic Changes of Gene Expression in *Arabidopsis* Polyploids. *Genetics*, **167**:1967-73.
- ³⁶ David W. Galbraith, Kristi R. Harkins, Joyce M. Maddox, Nicola M. Ayres, Dharam P. Sharma, and Ebrahim Firoozabadi (1983) Rapid Flow Cytometric Analysis of the Cell Cycle in Intact Plant Tissues. *Science*, **220**:1045-51

- ³⁷ Gerald Hall, J. R., George C. Allen, Deborah S. Loer, William F. Thompson, and Steven Spiker (1991) Nuclear scaffold and scaffold-attachment regions in higher plants. *Biochemistry*, **88**:9320-24.
- ³⁸ Anne Wang, Chin-Jen Wu, and Shu-Hui Chen (2006) Gold Nanoparticle, Assisted Protein Enrichment and Electroelution for Biological Samples. *Journal of Proteome Research*, **6**:1488-92.
- ³⁹ Sebastian Wiese, Kai A. Reidegeld, Helmut E. Meyer, Bettina Warscheid (2006) Protein labeling by iTRAQ: A new tool for quantitative mass spectrometry in proteome research. *Proteomics*, **7**:340-50.
- ⁴⁰ Pylatuik J. D. , Fobert P. R. (2005) Comparison of transcript profiling on *Arabidopsis* microarray platform technologies. *Plant Molecular Biology* **58**:609-24.
- ⁴¹ G. Jovtchev, V. Schubert, A. Meister, M. Barow, I. Schubert (2006) Nuclear DNA content and nuclear and cell volume are positively correlated in angiosperms. *Cytogenetic Genome Research*, **114**:77-82.
- ⁴² Schubert et al. (2006). Sister Chromatids Are Often Incompletely Aligned in Meristematic and Endopolyploid Interphase Nuclei of *Arabidopsis thaliana*. *Genetics*, **172**:467-475.
- ⁴³ R. L. Glaser, T.J. Leach and S.E. Ostrowski (1997) The Structure of Heterochromatic DNA Is Altered in Polyploid Cells of *Drosophila melanogaster*. *Molecular and Cellular Biology*, **17**:1254-63.
- ⁴⁴ Pauline E. Jullien, Tetsu Kinoshita, Nir Ohad and Frédéric Berger (2006) Maintenance of DNA Methylation during the *Arabidopsis* Life Cycle Is Essential for Parental Imprinting. *The Plant Cell*, **18**:1360-72.
- ⁴⁵ Oliver J. Ratcliffe and José Luis Riechmann (2002) *Arabidopsis* Transcription Factors and the Regulation of Flowering Time: A Genomic Perspective. *Current Issues In Molecular Biology*, **4**:77-91.
- ⁴⁶ Luisa Mariconti, Barbara Pellegrini, Rita Cantoni, Rebecca Stevens, Catherine Bergounioux, Rino Cell, and Diego Albani (2002) The E2F Family of Transcription Factors from *Arabidopsis thaliana*. *Journal of Biology and Chemistry*, **277**: 9911-19.
- ⁴⁷ Z. Jefferey Chen and Craig S. Pikaard (2003) Epigenetic silencing of RNA polymerase I transcription. *Genes and Development*, **4**:641-49.
- ⁴⁸ Singh B. N., Sopory S. K., Reddy M. K. (2004) Plant DNA Topoisomerases: Structure, Function, and Cellular Roles in Plant Development. *Critical Reviews In Plant Sciences*, **3**:251-69.

- ⁴⁹ Felipe Cortés and Nuria Pastor (2003) Induction of endoreduplication by topoisomerase II catalytic inhibitors. *Mutagenesis*, **18**:105-12.
- ⁵⁰ S Xie and E Lam (1994) Abundance of nuclear DNA topoisomerase II is correlated with proliferation in *Arabidopsis thaliana*. *Nucleic Acid Research*, **22**:5729-36.
- ⁵¹ Kevin D Corbett, Piero Benedetti, James M Berger (2007) Holoenzyme assembly and ATP-mediated conformational dynamics of topoisomerase VI. *Nature Structure and Molecular Biology*, **7**:611-19.
- ⁵² K Schneider, B Wells, L Dolan and K Roberts (1997) Structural and genetic analysis of epidermal cell differentiation in *Arabidopsis* primary roots. *Development*, **124**:1789-98.
- ⁵³ Yanhai Yin, Hyeonsook Cheong, Danielle Friedrichsen, Yunde Zhao, Jianping Hu, Santiago Mora-Garcia, and Joanne Chory (2002) A crucial role for the putative *Arabidopsis* topoisomerase VI in plant growth and development. *PNAS*, **15**:10191-96.
- ⁵⁴ Frank Hartung, Karel J Angelis, Armin Meister, Ingo Schubert, Michael Melzer and Holger Puchta (2002) An Archaeobacterial Topoisomerase Homolog Not present in Other Eukaryotes Is Indispensable for Cell proliferation of Plants. *Current Biology*, **12**:1787-91.
- ⁵⁵ Hulo N., Bairoch A., Bulliard V., Cerutti L., Cuče B., De Castro E., Lachaize C., Langendijk-Genevaux P.S., Sigrist C.J.A. (2007) The 20 years of PROSITE. *Nucleic Acids Research*.
- ⁵⁶ Russell Sambrook (2001) Molecular Cloning, *A laboratory Manual*, **3**:196-224.
- ⁵⁷ Fujikawa Y. and Kato N. (2007) Split luciferase complementation assay to study protein-protein interactions in *Arabidopsis* protoplasts. *The Plant Journal*, **52**:185-95.
- ⁵⁸ R.D. Finn, J. Tate, J. Mistry, P.C. Coggill, J.S. Sammut, H.R. Hotz, G. Ceric, K. Forslund, S.R. Eddy, E.L. Sonnhammer and A. Bateman (2008) Nucleic Acids Research Database Issue 36:D281-D288.

VITA

Rasheed Ahmad was born in Abu Dhabi, United Arab Emirates (UAE), in March, 1983. He attended Winona State University and completed his bachelor degree in cell and molecular biology in 2003. Rasheed worked as an account manager for Goldstar Wholesale from January 2004 to December 2005. He joined Dr. Naohiro Kato's lab at Louisiana State University in 2006 for his graduate studies. Once he has received his master degree in biochemistry in August 2009, Rasheed will join the MBA program at the University of Louisiana at Lafayette.